Hindawi Publishing Corporation
EURASIP Journal on Image and Video Processing
Volume 2008, Article ID 824726, 30 pages
doi:10.1155/2008/824726

*Research Article*

# A Review and Comparison of Measures for Automatic Video Surveillance Systems

**Axel Baumann, Marco Boltz, Julia Ebling, Matthias Koenig, Hartmut S. Loos, Marcel Merkel, Wolfgang Niem, Jan Karl Warzelhan, and Jie Yu**

*Corporate Research, Robert Bosch GmbH, D-70049 Stuttgart, Germany*

Correspondence should be addressed to Julia Ebling, julia.ebling@de.bosch.com

Received 30 October 2007; Revised 28 February 2008; Accepted 12 June 2008

Recommended by Andrea Cavallaro

Today's video surveillance systems are increasingly equipped with video content analysis for a great variety of applications. However, reliability and robustness of video content analysis algorithms remain an issue. They have to be measured against ground truth data in order to quantify the performance and advancements of new algorithms. Therefore, a variety of measures have been proposed in the literature, but there has neither been a systematic overview nor an evaluation of measures for specific video analysis tasks yet. This paper provides a systematic review of measures and compares their effectiveness for specific aspects, such as segmentation, tracking, and event detection. Focus is drawn on details like normalization issues, robustness, and representativeness. A software framework is introduced for continuously evaluating and documenting the performance of video surveillance systems. Based on many years of experience, a new set of representative measures is proposed as a fundamental part of an evaluation framework.



## 1. INTRODUCTION

The installation of videosurveillance systems is driven by the need to protect privateproperties, and by crime prevention, detection, and prosecution, particularly for terrorism in public places. However, the effectiveness of surveillance systems is still disputed [1]. One effect which is thereby often mentioned is that of crime dislocation. Another problem is that the rate of crime detection using surveillance systems is not known. However, they have become increasingly useful in the analysis and prosecution of known crimes.

Surveillance systems operate 24 hours a day, 7 days a week. Due to the large number of cameras which have to be monitored at large sites, for example, industrial plants, airports, and shopping areas, the amount of information to be processed makes surveillance a tedious job for the security personnel [1]. Furthermore, since most of the time video streams show ordinary behavior, the operator may become inattentive, resulting in missing events.

In the last few years, a large number of automatic real-time video surveillance systems have been proposed in the literature [2] as well as developed and sold by companies. The idea is to automatically analyze video streams and alert operators of potentially relevant security events. However, the robustness of these algorithms as well as their performance is difficult to judge. When algorithms produce too many errors, they will be ignored by the operator, or even distract the operator from important events.

During the last few years, several performance evaluation projects for video surveillance systems have been undertaken [3–9], each with different intentions. CAVIAR [3] addresses city center surveillance and retail applications. VACE [9] has a wide spectrum including the processing of meeting videos and broadcasting news. PETS workshops [8] focus on advanced algorithms and evaluation tasks like multiple object detection and event recognition. CLEAR [4] deals with people tracking and identification as well as pose estimation and face tracking while CREDS workshops [5] focus on event detection for public transportation security issues. ETISEO [6] studies the dependence between video characteristics and segmentation, tracking and event detection algorithms, whereas i-LIDS [7] is the benchmark system used by the UK Government for different scenarios like abandoned baggage, parked vehicle, doorway surveillance, and sterile zones.

Decisions on whether any particular automatic video surveillance system ought to be bought; objective quality measures, such as a false alarm rate, are required. This is important for having confidence in the system, and to decide whether it is worthwhile to use such a system. For the design and comparison of these algorithms, on the other hand, a more detailed analysis of the behavior is needed to facilitate a feeling of the advantages and shortcomings of different approaches. In this case, it is essential to understand the different measures and their properties.

Over the last years, many different measures have been proposed for different tasks; see, for example, [10–15]. In this paper, a systematic overview and evaluation of these measures is given. Furthermore, new measures are introduced, and details like normalization issues, robustness, and representativeness are examined. Concerning the significance of the measures, other issues like the choice and representativeness of the database used to generate the measures have to be considered as well [16].

In Section 2, ground truth generation and the choice of the benchmark data sets in the literature are discussed. A software framework to continuously evaluate and document the performance of video surveillance algorithms using the proposed measures is presented in Section 3. The survey of the measures can be found in Section 4 and their evaluation in Section 5, finishing with some concluding remarks in Section 6.

## 2. RELATED WORK

Evaluating performance of video surveillance systems requires a comparison of the *algorithm results* (*ARs*) with "optimal" results which are usually called *ground truth* (*GT*). Before the facets of *GT* generation are discussed (Section 2.2), a strategy which does not require *GT* is put forward (Section 2.1). The choice of video sequences on which the surveillance algorithms are evaluated has a large influence on the results. Therefore, the effects and peculiarities of the choice of the benchmark data set are discussed in Section 2.3.

### 2.1. Evaluation without ground truth

Erdem et al. [17] applied color and motion features instead of *GT*. They have to make several assumptions such as object boundaries always coinciding with color boundaries. Furthermore, the background has to be completely stationary or moving globally. All these assumptions are violated in many real world scenarios, however, the tedious generation of *GT* becomes redundant. The authors state that measures based on their approach produce comparable results to *GT*-based measures.

### 2.2. Ground truth

The requirements and necessary preparations to generate *GT* are discussed in the following subsections. In Section 2.2.1, file formats for *GT* data are presented. Different *GT* generation techniques are compared in Section 2.2.2, whereas Section 2.2.3 introduces *GT* annotation tools.

#### 2.2.1. File formats

For the task of performance evaluation, file formats for *GT* data are not essential in general but a common standardized file format has strong benefits. For instance, these include the simple exchange of *GT* data between different groups and easyintegration. A standard file format reduces the effort required to compare different algorithms and to generate *GT* data. Doubtlessly, a diversity of custom file formats exists among research groups and the industry. Many file formats in the literature are based on XML. The *computer vision markup language* (CVML) has been introduced by List and Fisher [18] including platform independent implementations. The PETS metric project [19] provides its own XML format which is used in the PETS workshops and challenges. The ViPER toolkit [20] employs another XML-based file format. A common, standardized, widely used file format definition providing a variety of requirements in the near future are doubtful as every evaluation program in the past introduced new formats and tools.

#### 2.2.2. Ground truth generation

A vital step prior to the generation of *GT* is the definition of annotation rules. Assumptions about the expected observations have to be made, for instance, how long does luggage have to be left unattended before an unattended luggage event is raised. This event might, for example, be raised as soon as the distance between luggage and person in question reaches a certain limit, or when the person who left the baggage leaves the scene and does not return for at least sixty seconds. ETISEO [6] and PETS [8] have made their particular definitions available on their websites. As with file formats, a common annotation rule definition does not exist. This complicates the performance evaluation between algorithms of different groups.

Three types of different approaches are described in the literature to generate *GT*. Semiautomatic *GT* generation is proposed by Black et al. [11]. They incorporate the video surveillance system to generate the *GT*. Only tracks with low object activity, as might be taken from recordings during weekends, are used. These tracks are checked for path, color, and shape coherence. Poor quality tracks are removed. The accepted tracks build the basis of a video subset which is used in the evaluation. Complex situations such as dynamic occlusions, abandoned objects, and other real-world scenarios are not covered by this approach. Ellis [21] suggests the use of synthetic image sequences. *GT* would then be known a priori, and tedious manual labeling is avoidable. Recently, Taylor et al. [22] propose a freely usable extension of a game engine to generate synthetic video sequences including pixel accurate *GT* data. Models for radial lens distortion, controllable pixel noise levels, and video ghosting are some of the features of the proposed system. Unfortunately, even the implementation of a simple screenplay requires an expert in level design and takes a lot

of time. Furthermore, the applicability of such sequences to real-world scenarios is unknown. A system which works well on synthetic data does not necessarily work equally well on real-world scenarios.

Due to the limitations of the previously discussed approaches, the common approach is the tedious labor-intensive manual labeling of every frame. While this task can be done relatively quickly for events, a pixel accurate object mask for every frame is simply not feasible for complete sequences. A common consideration is to label on a bounding box level. Pixel accurate labeling is done only for predefined frames, like every 60th frame. Young and Ferryman [13] state that different individuals produce different *GT* data of the same video. To overcome this limitation, they suggest to let multiple humans label the same sequence and use the "average" of their results as *GT*. Another approach is labeling the boundaries of object masks as an own category and exclude this category in the evaluation [23]. List et al. [24] let three humans annotate the same sequence and compared the result. About 95% of the data matched. It is therefore unrealistic to demand a perfect match between *GT* and *AR*. The authors suggest that when more than 95% of the areas overlap, then the algorithm should be considered to have succeeded. Higher level ground truth like events can either be labeled manually, or be inferred from a lower level like frame-based labeling of object bounding boxes.

#### 2.2.3. Ground truth annotation tools

A variety of annotation tools exist to generate *GT* data manually. Commonly used and freely available is the ViPER-GT [20] tool (see Figure 1), which has been used, for example, in the ETISEO [6] and the VACE [9] projects. The CAVIAR project [3] used an annotation tool based on the AviTrack [25] project. This tool has been adapted for the PETS metrics [19]. The ODViS project [26] provides its own *GT* tool. All of the above-mentioned *GT* annotation tools are designed to label on a bounding box basis and provide support to label events. However, they do not allow the user to label the data at a pixel-accurate level.

### 2.3. Benchmark data set

Applying an algorithm to different sequences will produce different performance results. Thus, it is inadequate to evaluate an algorithm on a single arbitrary sequence. The choice of the sequence set is very important for the meaningful evaluation of the algorithm performance. Performance evaluation projects for video surveillance systems [3–9] therefore provide a benchmark set of annotated video sequences. However, the results of the evaluation still depend heavily on the chosen benchmark data set.

The requirements of the video processing algorithms depend heavily on the type of scene to be processed. Examples for different scenarios range from sterile zones including fence monitoring, doorway surveillance, parking vehicle detection, theft detection, to abandoned baggage in crowded scenes like public transport stations. For each

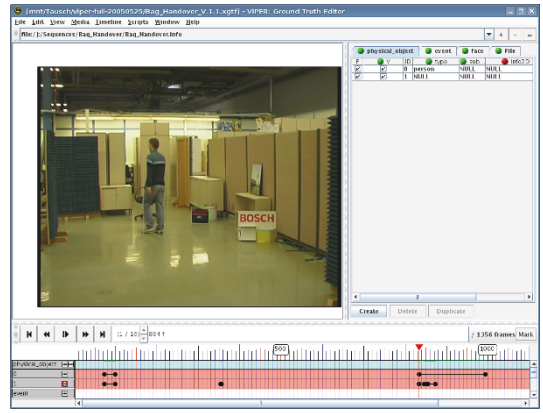


Figure 1: Freely available ground truth annotation tool Viper-GT [20].

of these scenarios, the surveillance algorithms have to be evaluated separately. Most of the evaluation programs focus on only a few of these scenarios.

To gain more granularity, the majority of these evaluation programs [3–5, 8, 9] assign sequences to different levels of difficulty. However, they do not take the step to declare due to which video processing problems these difficulty levels are reached. Examples for challenging situations in video sequences are a high-noise level, weak contrasts, illumination changes, shadows, moving branches in the background, the size and amount of objects in the scene, and different weather condition. Further insight into the particular advantages and disadvantages of different video surveillance algorithms is hindered by not studying these problems separately.

ETISEO [6], on the other hand, also studies the dependencies between algorithms and video characteristics. Therefore, they propose an evaluation methodology that isolates video processing problems [16]. Furthermore, they define quantitative measures to define the difficulty level of a video sequence with respect to the given problem. The highest difficulty level for a single video processing problem an algorithm can cope with can thus be estimated.

The video sequences used in the evaluations are typically in the range of a few hundred to some thousand frames. With a typical frame rate of about 12 frames per second, a sequence with 10000 frames is approximately 14 minutes long. Comparing this to the real-world utilization of the algorithms which requires 24/7 surveillance including the changes from day to night, as well as all weather conditions for outdoor applications, raises the question of how representative the short sequences used in evaluations really are. This question is especially important as many algorithms include a learning phase and continuously learn and update the background to cope with the changing recording conditions [2]. i-LIDS [7] is the first evaluation to use long sequences with hours of recording of realistic scenes for the benchmark data set.

## 3. EVALUATION FRAMEWORK

To control the development of a video surveillance system, the effects of changes to the code have to be determined and

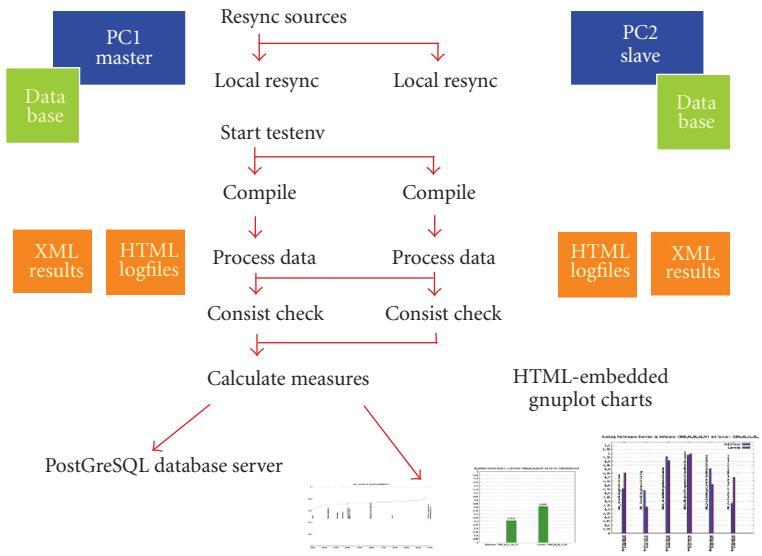


Figure 2: Schematic workflow of the automatic test environment.

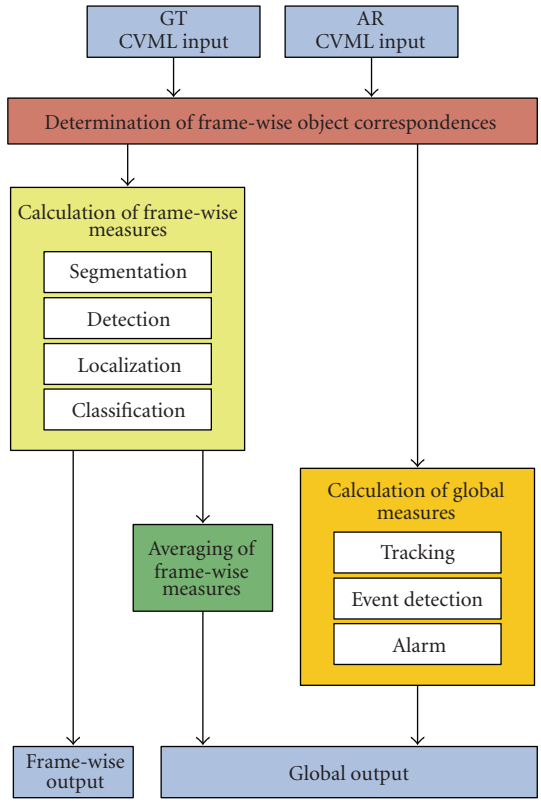


Figure 3: Workflow of the measure tool. The main steps are the reading of the data to compare, the determination of the correspondences between *AR* and *GT* objects, the calculation of the measures, and finally the output of the measure values.

evaluated regularly. Thereby modifications to the software are of interest as well as changes to the resulting performance. When changing the code, it has to be checked whether the software still runs smoothly and stable, and whether changes of the algorithms had the desired effects to the performance of the system. If, for example, after changing the code no changes of the system output are anticipated, this has to be verified with the resulting output. The algorithm performance, on the other hand, can be evaluated with the measures presented in this paper.

As the effects of changes of the system can be quite different in relation to the processed sequences, preferably a large number of different sequences should be used for the examination. The time and effort of conducting numerous tests for each code change by hand are much too large, which leads to assigning these tasks to an automatic test environment (ATE).

In the following subsections, such an evaluation framework is introduced. A detailed system setup is described in Section 3.1, and the corresponding system work flow is presented in Section 3.2. In Section 3.3, the computation framework of the measure calculation can be found. The preparation and presentation of the resulting values are outlined in Section 3.4. Figure 2 shows an overview of the system.

### 3.1. System setup

The system consists of two computers operating in synchronized work flow: a Windows Server system acting as the slave system and a Linux system as the master (see Figure 2). Both systems feature identical hardware components. They are state-of-the-art workstations with dual quad-core Xeon processors and 32 GB memory. They are capable of simultaneously processing 8 test sequences under full usage of processing power. The sources are compiled with commonly used compilers GCC 4.1 on the Linux system and Microsoft Visual Studio 8 on the Windows system. Both systems are necessary as the development is either done on Windows or Linux and thus consistency checks are necessary on both systems.

### 3.2. Work flow

The ATE permanently keeps track of changes to the source code version management. It checks for code changes and when these occur, it starts with resyncing all local sources to their latest versions and compiling the source code. In the event of compile errors of essential binaries preventing a complete build of the video surveillance system, all developers are notified by an email giving information about the changes and their authors. Starting the compile process on both systems provides a way of keeping track of compiler-dependent errors in the code that might not attract attention when working and developing with only one of the two systems.

At regular time intervals (usually during the night, when major code changes have been committed to the version management system), the master starts the algorithm performance evaluation process. After all compile tasks completed successfully, a set of more than 600 video test sequences including subsets of the CANDELA [27], CAVIAR [3], CREDS [5], ETISEO [6], i-LIDS [7], and PETS [8] benchmark data sets is processed by the built binaries on both systems. All results are stored in a convenient way for further evaluation.

After all sequences have been processed, the results of these calculations are evaluated by the measure tool (Section 3.3). As this tool is part of the source code, it is also updated and compiled for each ATE process.

### 3.3. Measure tool

The measure tool compares the results from processing the test sequences with ground truth data and calculates measures describing the performance of the algorithm. Figure 3 shows the workflow. For every sequence, it starts with reading the CVML [18] files containing the data to be compared. The next step is the determination of the correspondences between *AR* and *GT* objects, which is done frame by frame. Based on these correspondences, the frame-wise measures are calculated and the values stored in an output file. After processing the whole sequence, the frame-wise measures are averaged and global measures like tracking measures are calculated. The resulting sequence-based measure values are stored in a second output file.

The measure tool calculates about 100 different measures for each sequence. Taking into account all included variations, their number raises to approximately 300. The calculation is done for all sequences with *GT* data, which are approximately 300 at the moment. This results in about 90000 measure values for one ATE run not including the frame-wise output.

### 3.4. Preparation and presentation of results

In order to easily access all measure results, which represent the actual quality of the algorithms, they are stored in a relational database system. The structured query language (SQL) is used as it provides very sophisticated ways of querying complex aspects and correlations between all measure values associated with sequences and the time they were created.

In the end, all results and logging information about success, duration, problems, or errors of the ATE process are transferred to a local web server that shows all this data in an easily accessible way including a web form to select complex parameters to query the SQL database. These parts of the ATE are scripted processes implemented in Perl.

When selecting query parameters for evaluating measures, another Perl/CGI-script is being used. Basically, it compares the results of the current ATE pass with a previously set reference version which usually represents a certain point in the development where achievements were made or an error-free state had been reached. The query provides an evaluation of results for single selectable measures over a certain time in the past, visualizing data by plotted graphs and emphasizing various deviations between current and reference versions and improvements or deteriorations of results.

The ATE was build in 2000 and since then, it runs nightly and whenever the need arises. In the last seven years, this accumulated to over 2000 runs of the ATE. Started with only the consistency checks and a small set of metrics without additional evaluations, the ATE grew to a powerful tool providing meaningful information presented in a well arranged way. Lots of new measures and sequences have been added over time so that new automatic statistical evaluations to deal with the mass of produced data had to be integrated. Further information about statistical evaluation can be found in Section 5.4.

## 4. METRICS

This section introduces and discusses metrics for a number of evaluation tasks. First of all, some basic notations and measure equations are introduced (Section 4.1). Then, the issue of matching algorithm result objects to ground truth objects and vice versa is discussed (Section 4.2). Structuring of the measures themselves is done according to the different evaluation tasks like segmentation (Section 4.3), object detection (Section 4.4), and localization (Section 4.5), tracking (Section 4.6), event detection (Section 4.7), object classification (Section 4.8), 3D object localization (Section 4.9), and multicamera tracking (Section 4.10). Furthermore, several issues and pitfalls of aggregating and averaging measure values to obtain single representative values are discussed (Section 4.11).

In addition to metrics described in the literature, custom variations are also listed, and a selection based on their usefulness is made. There are several criteria influencing the choice of metrics to be used, including the use of only normalized metrics where a value of 0 represents the worst and a value of 1 the best result. This normalization provides a chance for unified evaluations.

### 4.1. Basic notions and notations

Let *GT* denote the ground truth and *AR* the result of the algorithm. True positives (*TPs*) relate to elements belonging

Table 1: Frequently used notations. (a) basic abbreviations. (b) indices to distinguish different kinds of result elements. An element could be a frame, a pixel, an object, a track, or an event. (c) some examples.

(a) Basic abbreviations

| | |
|---|---|
| *GT* | Ground truth element |
| *AR* | Algorithm result element |
| *FP* | False positive, an element present in *AR*, but not in *GT* |
| *FN* | False negative, an element present in *GT*, but not in *AR* |
| *TP* | True positive, an element present in *GT* and *AR* |
| *TN* | True negative, an element neither present in *GT* nor *AR* |
| # | number of |
| → | Left element assigned to right element |

(b) Subscripts to denote different elements

| Element | Index | Used counter |
|---|---|---|
| Frame | $f$ | $j$ |
| Pixel | $p$ | $k$ |
| Object | $o$ | $l$ |
| Track | tr | $i$ |
| Event | $e$ | $m$ |

(c) Examples

| | |
|---|---|
| $\#\mathrm{GT}_o$ | Number of objects in ground truth |
| $\#\mathrm{GT}_f$ | Number of frames containing at least one $\mathrm{GT}_o$ |
| $\#(\mathrm{GT}_{\mathrm{tr}} \rightarrow \mathrm{AR}_{\mathrm{tr}}(i))$ | Number of *GT* tracks which are assigned to the $i$th *AR* track |

to both *GT* and *AR*. False positive (*FP*) elements are those which are set in *AR* but not in *GT*. False negatives (*FNs*), on the other hand, are elements in the *GT* which are not in the *AR*. True negatives (*TNs*) occur neither in the *GT* nor in the *AR*. Please note that while true negative pixels and frames are well defined, it is not clear what a true negative object, track, or event should be. Depending on the type of regarded element—a frame, a pixel, an object, a track, or an event—a subscript will be added (see Table 1).

The most common measures precision, sensitivity (which is also called recall in the literature), and F-score count the number of *TP*, *FP*, and *FN*. They are used in small variation for many different tasks and will thus occur many more times in this paper. For clarity and reference, the standard formulas are presented here. Note that counts are represented by a #.

### *Precision (Prec)*

Measures the number of false positives:

$$\mathrm{Prec} = \frac{\#\mathrm{TP}}{\#\mathrm{TP} + \#\mathrm{FP}}. \tag{1}$$

### *Sensitivity (Sens)*

Measures the number of false negatives. Synonyms in literature are true positive rate (TPR), recall and hit rate

$$\mathrm{Sens} = \frac{\#\mathrm{TP}}{\#\mathrm{TP} + \#\mathrm{FN}}. \tag{2}$$

### *Specificity (Spec)*

The number of false detections in relation to the total number of negatives. Also called true negative rate (TNR)

$$\mathrm{Spec} = \frac{\#\mathrm{TN}}{\#\mathrm{TN} + \#\mathrm{FP}}. \tag{3}$$

Note that Spec should only be used for pixels or frame elements as true negatives are not defined otherwise.

### *False positive rate (FPR)*

The number of negative instances that were erroneously reported as being positive:

$$\mathrm{FPR} = \frac{\#\mathrm{FP}}{\#\mathrm{FP} + \#\mathrm{TN}} = 1 - \mathrm{Spec}. \tag{4}$$

Please note that true negatives are only well defined for pixel or frame elements.

### *False negative rate (FNR)*

The number positive instances that were erroneously reported as negative:

$$\mathrm{FNR} = \frac{\#\mathrm{FN}}{\#\mathrm{FN} + \#\mathrm{TP}} = 1 - \mathrm{Sens}. \tag{5}$$

### *F-Measure*

Summarizes Prec and Sens by weighting their effect with the factor $\alpha$. This allows the F-Measure to emphasize one of the two measures depending on the application

$$\begin{aligned}\text{F-Measure} &= \frac{1}{\alpha \cdot (1/\mathrm{Sens}) + (1-\alpha)\cdot(1/\mathrm{Prec})} \\ &= \frac{\#\mathrm{TP}}{\#\mathrm{TP} + \alpha \cdot \#\mathrm{FN} + (1-\alpha)\cdot\#\mathrm{FP}}.\end{aligned} \tag{6}$$

### *F-Score*

In many applications the Prec and Sens are of equal importance. In this case, $\alpha$ is set to 0.5 and called F-Score which is in this case the the harmonic mean of Prec and Sens:

$$\text{F-Score} = \frac{2\cdot \mathrm{Prec}_{\mathrm{seg}} \cdot \mathrm{Sens}_{\mathrm{seg}}}{\mathrm{Prec}_{\mathrm{seg}} + \mathrm{Sens}_{\mathrm{seg}}} = \frac{\#\mathrm{TP}}{\#\mathrm{TP} + (1/2)(\#\mathrm{FN} + \#\mathrm{FP})}. \tag{7}$$

Usually, systems provide ways to optimize certain aspects of performance by using an appropriate configuration or

parameterization. One way to approach such an optimization is the receiver operation curve (ROC) optimization [28] (Figure 4). ROCs graphically interpret the performance of the decision-making algorithm with regard to the decision parameter by plotting TPR (also called Sens) against FPR. Each point on the curve is generated for the range of decision parameter values. The optimal point is located on the upper left corner $(0, 1)$ and represents a perfect result.

As Lazarevic-McManus et al. [29] point out, an object-based performance analysis does not provide essential true negative objects, and thus ROC optimization cannot be used. They suggest to use the F-Measure when ROC optimization is not appropriate.

### 4.2. Object matching

Many object- and track-based metrics, as will be presented, for example, in Sections 4.4, 4.5, and 4.6, assign *AR* objects to specific *GT* objects. The method and quality used for this matching greatly influence the results of the metrics based on these assignments.

In this section, different criteria found in the literature to fulfill the task of matching *AR* and *GT* objects are presented and compared using some examples. First of all, assignments based on evaluating the objects centroids are described in Section 4.2.1, then the object area overlaps and other matching criteria based on this are presented in Section 4.2.2.

#### 4.2.1. Object matching approach based on centroids

Note that distances are given within the definition of the centroid-based matching criteria. The criterion itself is gained by applying a threshold to this distance. When the distances are not binary, using thresholds involves the usual problems with choosing the right threshold value. Thus, the threshold should be stated clearly when talking about algorithm performance measured based on thresholds.

Let $\vec{b}_{\mathrm{GT}}$ be the bounding box of an *GT* object with centroid $\vec{x}_{\mathrm{GT}}$ and let $d_{\mathrm{GT}}$ be the length of the bounding box' diagonal of the *GT* object. Let $\vec{b}_{\mathrm{AR}}$ and $\vec{x}_{\mathrm{AR}}$ be the bounding box and the centroid of an *AR* object.

*Criterion 1.* A first criterion is based on the thresholded Euclidean distance between the object's centroids, and can be found for instance in [14, 30]

$$D_1 = \left|\vec{x}_{\mathrm{GT}} - \vec{x}_{\mathrm{AR}}\right|. \tag{8}$$

*Criterion 2.* A more advanced version is given by normalizing the diagonal of the *GT* object's bounding box:

$$D_2 = \frac{\left|\vec{x}_{\mathrm{GT}} - \vec{x}_{\mathrm{AR}}\right|}{d_{\mathrm{GT}}}. \tag{9}$$

Another method to determine assignments between *GT* and *AR* objects checks if the centroid $\vec{x}_i$ of one bounding box $\vec{b}_i$ lies inside the other. Based on this idea, different criteria can be derived.

*Criterion 3.*

$$D_3 = \begin{cases} 0: & \vec{x}_{\mathrm{GT}} \text{ is inside } \vec{b}_{\mathrm{AR}}, \\ 1: & \text{else.} \end{cases} \tag{10}$$

*Criterion 4* (e.g., [30]).

$$D_4 = \begin{cases} 0: & \vec{x}_{\mathrm{AR}} \text{ is inside } \vec{b}_{\mathrm{GT}}, \\ 1: & \text{else.} \end{cases} \tag{11}$$

*Criterion 5.*

$$D_5 = \begin{cases} 0: & \vec{x}_{\mathrm{GT}} \text{ is inside } \vec{b}_{\mathrm{AR}}, \text{or } \vec{x}_{\mathrm{AR}} \text{ is inside } \vec{b}_{\mathrm{GT}}, \\ 1: & \text{else.} \end{cases} \tag{12}$$

*Criterion 6* (e.g., [30]).

$$D_6 = \begin{cases} 0: & \vec{x}_{\mathrm{GT}} \text{ is inside } \vec{b}_{\mathrm{AR}}, \text{ and } \vec{x}_{\mathrm{AR}} \text{ is inside } \vec{b}_{\mathrm{GT}}, \\ 1: & \text{else.} \end{cases} \tag{13}$$

*Criterion 7.* An advancement of the Criterion 6 uses the distances $d_{\mathrm{GT,AR}}$ and $d_{\mathrm{AR,GT}}$ from the centroid of one object to the closest point of the bounding box of the other object [10]. The distance is 0 if Criterion 6 is fulfilled,

$$D_7 = \begin{cases} 0: & \vec{x}_{\mathrm{GT}} \text{ is inside } \vec{b}_{\mathrm{AR}}, \\ & \text{and } \vec{x}_{\mathrm{AR}} \text{ is inside } \vec{b}_{\mathrm{GT}}, \\ \min(d_{\mathrm{GT,AR}}, d_{\mathrm{AR,GT}}): & \text{else,} \end{cases} \tag{14}$$

where $d_{k,l}$ is the distance from the centroid $\vec{x}_k$ to the closest point of the bounding box $\vec{b}_l$ (see Figure 5).

*Criterion 8.* A criterion similar to Criterion 7 but based on Criterion 5 instead of Criterion 6:

$$D_8 = \begin{cases} 0: & \vec{x}_{\mathrm{GT}} \text{ is inside } \vec{b}_{\mathrm{AR}}, \\ & \text{or } \vec{x}_{\mathrm{AR}} \text{ is inside } \vec{b}_{\mathrm{GT}}, \\ \min(d_{\mathrm{GT,AR}}, d_{\mathrm{AR,GT}}): & \text{else.} \end{cases} \tag{15}$$

*Criterion 9.* Using the minimal distance affects some drawbacks, which will be discussed later, we tested another variation based on Criterion 7, which uses the average of the two distances:

$$D_9 = \begin{cases} 0: & \vec{x}_{\mathrm{GT}} \text{ is inside } \vec{b}_{\mathrm{AR}}, \\ & \text{and } \vec{x}_{\mathrm{AR}} \text{ is inside } \vec{b}_{\mathrm{GT}}, \\ \dfrac{d_{\mathrm{GT,AR}} + d_{\mathrm{AR,GT}}}{2}: & \text{else.} \end{cases} \tag{16}$$

The above-mentioned methods to perform matching between *GT* and *AR* objects via the centroid's position are relatively simple to implement and incur low calculation costs. Methods using a distance threshold have the disadvantage of being influenced by the image resolution of the video

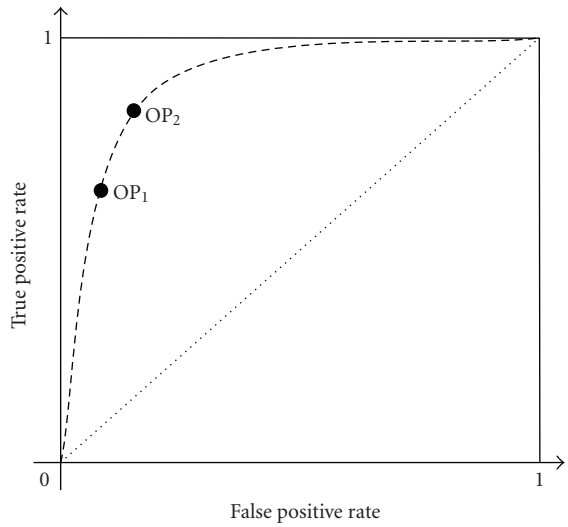


Figure 4: One way to approach an optimization of an algorithm is the receiver operation curve (ROC) optimization [28, 31]. ROCs graphically interpret the performance of the decision making algorithm with regard to the decision parameter by plotting TPR (also called Sens) against FPR. The points $OP_1$ and $OP_2$ show two examples of possible operation points.

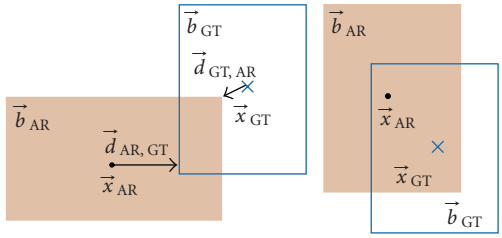


Figure 5: Bounding box distances $\vec{d}_{GT,AR}$ and $\vec{d}_{AR,GT}$ in two simple examples. Blue bounding boxes relate to *GT*, whereas orange bounding boxes relate to *AR*. A bounding box is quoted by $\vec{b}$, the centroid of the bounding box is quoted by $\vec{x}$.

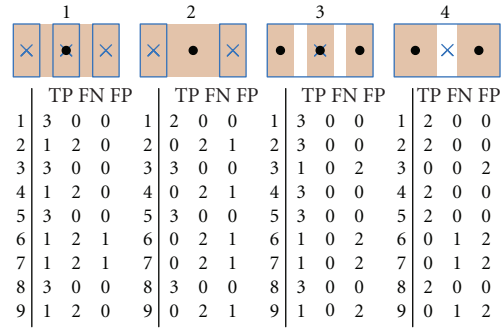


| | TP | FN | FP | | TP | FN | FP | | TP | FN | FP | | TP | FN | FP |
|---|---|---|---|---|---|---|---|---|---|---|---|---|---|---|---|
| 1 | 3 | 0 | 0 | 1 | 2 | 0 | 0 | 1 | 3 | 0 | 0 | 1 | 2 | 0 | 0 |
| 2 | 1 | 2 | 0 | 2 | 0 | 2 | 1 | 2 | 3 | 0 | 0 | 2 | 2 | 0 | 0 |
| 3 | 3 | 0 | 0 | 3 | 3 | 0 | 0 | 3 | 1 | 0 | 2 | 3 | 0 | 0 | 2 |
| 4 | 1 | 2 | 0 | 4 | 0 | 2 | 1 | 4 | 3 | 0 | 0 | 4 | 2 | 0 | 0 |
| 5 | 3 | 0 | 0 | 5 | 3 | 0 | 0 | 5 | 3 | 0 | 0 | 5 | 2 | 0 | 0 |
| 6 | 1 | 2 | 1 | 6 | 0 | 2 | 1 | 6 | 1 | 0 | 2 | 6 | 0 | 1 | 2 |
| 7 | 1 | 2 | 1 | 7 | 0 | 2 | 1 | 7 | 1 | 0 | 2 | 7 | 0 | 1 | 2 |
| 8 | 3 | 0 | 0 | 8 | 3 | 0 | 0 | 8 | 3 | 0 | 0 | 8 | 2 | 0 | 0 |
| 9 | 1 | 2 | 0 | 9 | 0 | 2 | 1 | 9 | 1 | 0 | 2 | 9 | 0 | 1 | 2 |

Figure 6: Examples for split and merge situations. The *GT* object bounding boxes are shown in blue with a cross at the object center and the *AR* in orange with a black dot at the object center. Depending on the matching Criteria (1–9), different numbers of *TP*, *FN*, and *FP* are computed for the chosen situations.

input, if the *AR* or *GT* data is not normalized to a specified resolution. One way to avoid this drawback is to append a normalization factor as shown in Criterion 2 or to check only whether a centroid lies inside an area or not. Criteria based on the distance from the centroid of one object to the edge of the bounding box of the other object instead of the Euclidean distance between the centroids have the advantage that there are no skips in split and merge situations.

However, the biggest drawback of all above-mentioned criteria is their inability to perform reliable correspondences between *GT* and *AR* objects in complex situations. This implies undesirable results in split and merge situations as well as permutations of assignments in case of objects occluding each other. These problems will be clarified by means of some examples below. The examples show diverse constellations of *GT* and *AR* objects, where *GT* objects are represented by bordered bounding boxes with a cross as centroid and the *AR* objects by frameless filled bounding boxes with a dot as centroid. Under each constellation, a table lists the numbers of *TP*, *FN*, and *FP* for the different criteria.

Example 1 (see Figure 6) shows a typical merge situation in which a group of three objects is merged in one blob. The centroid of the middle object exactly matches the centroid of the *AR* bounding box. Regarding the corresponding table, one can see that Criterion 1, Criterion 3, Criterion 5, and Criterion 8 rate all the *GT* objects as detected and, in contrast, Criterion 4 and Criterion 6 only the middle. Criterion 1 would also results in the latter when the distance from the outer *GT* centroids to the *AR* centroid exceeds the defined threshold. Furthermore, Criterion 7 and Criterion 9 penalize the outer objects, depending on the thresholds, if they are successful detections.

Example 2 (see Figure 6) represents a similar situation but with only two objects located in a certain distance from each other. The *AR* merges these two *GT* objects, which could be caused for example by shadows. Contrary to Example 1, the middle of the *AR* bounding box is not covered by a *GT* bounding box, so that Criterion 4 and Criterion 6 are not fulfilled, hence it is penalized with 2 *FN* and one *FP*. Note that the additional *FP* causes a worse performance measure than when the *AR* contained no object.

Problems in split situations follow a similar pattern. Imagine a scenario such as Example 3 (see Figure 6): a vehicle with 2 trailers appearing as 1 object in *GT*. But the system detects 3 separate objects. Or Example 4 (see Figure 6): a vehicle with only 1 trailer is marked as 2 separate objects. In these cases, *TP*s do not represent the number of successfully detected *GT* objects as usual, but successfully detected *AR* objects.

The fifth example (see Figure 7) shows the scenario of a car stopping, a person opening the door and getting off the vehicle. Objects to be detected are therefore the car and the person. Recorded *AR* shows, regarding the car, a bounding box being slightly too large (due to its shadow), and for the person a bounding box that stretches too far to the left. This typically occurs due to the moving car door, which cannot be separated from the person by the system. This example demonstrates how, due to identical distance values between

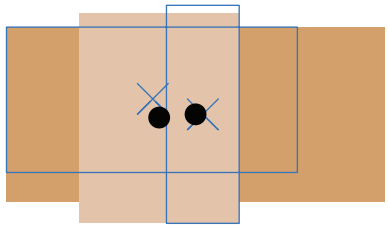

Figure 7: Example 5: person getting out of a car. The positions of the object centroids lead to assignment errors as the *AR* persons centroid is closer to the centroid of the car in the *GT* and vice versa. The *GT* object bounding boxes are shown in blue with a cross at the object center and the *AR* in orange with a black dot at the object center.

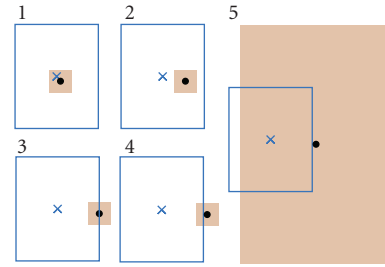


| Criterion | 1 | 2 | 3 | 4 | 5 |
|---|---|---|---|---|---|
| 7 | 0 | $d_{72}$ | 0 | $\approx 0$ | $\approx 0$ |
| 8 | 0 | 0 | 0 | $\approx 0$ | $\approx 0$ |
| 9 | 0 | $d_{92}$ | $d_{93} \approx d_{92}$ | $d_{94} \approx d_{93}$ | $d_{95} \approx d_{94}$ |

Figure 8: Drawbacks of matching Criterion 7 to Criterion 9. Five different configurations are shown to demonstrate the behavior of these criteria. The *GT* object bounding boxes are shown in blue with a cross at the object center and the *AR* in orange with a black dot at the object center. The distances $d_{\text{crit,conf}}$ of possible *GT*-*AR* combinations as computed by the Criterion 7 to Criterion 9 are either zero or identical to the distances of the other examples through these distances are visually different.

*GT*-*AR* object combinations, the described methods lack a decisive factor or even result in misleading distance values. The latter is the case, for example, Criterion 1 and Criterion 2, because the *AR* centroid of the car is closer to the centroid of the *GT* person, rather than the *GT* car, and vice versa.

Criterion 3 and Criterion 5 are particularly unsuitable, because there is no way to distinguish between a comparably harmless merge and cases where the detector identifies large sections of the frame as one object due to global illumination changes. Criterion 4 and Criterion 6 are rather generous when the *AR* object covers only fractions of the *GT* object. This is because a *GT* object is rated to be detected as soon as a smaller *AR* object (according to the size of the *GT* object) covers it.

Figure 8 illustrates the drawback of Criterion 7, Criterion 8, and Criterion 9. This is due to the fact that for the human eye quality wise different detection results cannot be distinguished by the given criteria. This leads to problems especially when multiple objects are located very close to each other and distances of possible *GT*/*AR* combinations are identical. Figure 8 shows five different patterns of one *GT* and one *AR* object as well as the distance values for the three chosen criteria. In the table in Figure 8, it can be seen that only Criterion 9 allows a distinct discrimination between configuration 1 and the other four. Furthermore, it can be seen that using Criterion 7, configuration 2 gets a worse distance value than configuration 3. Aside these two cases, the mentioned criteria are incapable of distinguishing between the five paradigmatic structures.

The above-mentioned considerations demonstrate the capability of the centroid-based criteria to represent simple and quick ways of assigning *GT* and *AR* objects to each other in test sequences with discrete objects. However, in complex problems such as occlusions or split and merge, their assignments are rather random. Thus, the content of the test sequence influences the quality of the evaluation results. While replacing object assignments has no effect on the detection performance measures, it impacts strongly on the tracking measures, which are based on these assignments, to.

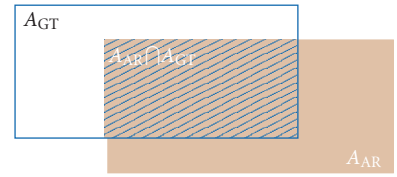


Figure 9: The area distance computes the overlap of the *GT* and *AR* bounding boxes.

#### 4.2.2. *Object matching based on object area overlap*

A reliable method to determine object assignments is provided by area distance calculation based on overlapping bounding box areas (see Figure 9).

*Frame detection accuracy (FDA) [32]*

Computes the ratio of the spatial intersection between two objects and their spatial union for one single frame:

$$\text{FDA} = \frac{\text{overlap}(\text{GT}, \text{AR})}{(1/2)(\#\text{GT}_o + \#\text{AR}_o)}, \tag{17}$$

where again $\#\text{GT}_o$ is the number of *GT* objects for a given frame ($\#\text{AR}_o$ accordingly). The overlap ratio is given by

$$\text{overlap}(\text{GT}, \text{AR}) = \sum_{l=1}^{\#(\text{AR}_o \to \text{GT}_o)} \frac{|A_{\text{GT}}(l) \cap A_{\text{AR}}(l)|}{|A_{\text{GT}}(l) \cup A_{\text{AR}}(l)|}. \tag{18}$$

Here, $\#(\text{AR}_o \to \text{GT}_o)$ is the number of mapped objects in frame $t$, by mapping objects according to their best spatial overlap (which is a symmetric criterion and thus $\#(\text{AR}_o \to \text{GT}_o) = \#(\text{GT}_o \to \text{AR}_o)$), $A_{\text{GT}}$ is the ground truth object area and $A_{\text{AR}}$ is the detected object area by an algorithm respectively.

*Overlap ratio thresholded (ORT) [32]*

This metric takes into account a required spatial overlap between the objects. The overlap is defined by a minimal threshold:

$$\mathrm{ORT} = \sum_{l=1}^{\#(\mathrm{AR}_o \to \mathrm{GT}_o)} \frac{\mathrm{OT}(A_{\mathrm{GT}}(l), A_{\mathrm{AR}}(l))}{|A_{\mathrm{GT}}(l) \cup A_{\mathrm{AR}}(l)|},$$

$$\mathrm{OT}(A_1, A_2) = \begin{cases} |A_1 \cup A_2|, & \text{if } \dfrac{|A_1 \cap A_2|}{|A_1|} \geq \text{threshold}, \\ |A_1 \cap A_2|, & \text{otherwise.} \end{cases} \tag{19}$$

Again, $\#(\mathrm{AR}_o \to \mathrm{GT}_o)$ is the number of mapped objects in frame $t$, by mapping objects according to their best spatial overlap, $A_{\mathrm{GT}}$ is the ground truth object area and $A_{\mathrm{AR}}$ is the detected object area by an algorithm.

*Sequence frame detection accuracy (SFDA) [32]*

Is a measure that extends the *FDA* to the whole sequence. It uses the *FDA* for all frames and is normalized to the number of frames where at least one *GT* or *AR* object is detected in order to account for missed objects as well as false alarms:

$$\mathrm{SFDA} = \frac{\sum_{j=1}^{\#\mathrm{frames}} \mathrm{FDA}(j)}{\#\{\mathrm{frames} | (\#\mathrm{GT}_o(j) > 0) \vee (\#\mathrm{AR}_o(j) > 0)\}}. \tag{20}$$

In a similar approach, [33] calculates values for recall and precision and combines them by a harmonic mean in the F-measure for every pair of *GT* and *AR* objects. The F-measures are then subjected to the thresholding step and finally leading to false positive and false negative rates. In the context of the ETISEO benchmarking, Nghiem et al. [34] tested different formulas for calculating the distance value and come to the conclusion that the choice of matching functions does not greatly affect the evaluation results. The dice coefficient function (D1) is the one chosen, which leads to the same matching function [33] used by the so-called F-measure.

First of all, the dice coefficient is calculated for all *GT* and *AR* object combinations:

$$\mathtt{D1} = \frac{2 \cdot \#(\mathrm{GT}_o \cap \mathrm{AR}_o)}{\#\mathrm{GT}_o + \#\mathrm{AR}_o}. \tag{21}$$

After thresholding, the assignment commences, in which no multiple correspondences are allowed. So in case of multiple overlaps, the best overlap becomes a correspondence, turning unavailable for further assignments. Since this approach does not feature the above-mentioned drawbacks, we decided to determine object correspondences via the overlap.

### 4.3. Segmentation measures

The segmentation step in a video surveillance system is critical as its results provide the basis for successive steps and thus influence the performance in subsequent steps. The evaluation of segmentation quality has been an active research topic in image processing, and various measures have been proposed depending on the application of the segmentation method [35, 36]. In the considered context of evaluating video surveillance systems, the measures fall into the category of discrepancy methods [36] which quantify differences between an actually segmented (observed) image and a ground truth. The most common segmentation measures precision, sensitivity, and specificity consider the area of overlap between *AR* and *GT* segmentation. In [15], the bounding box areas and not the filled pixel contours are pixel-wise taken into account to get the numbers of true positives (*TPs*), false positives (*FPs*), and false negatives (*FNs*) (see Figure 10) and to define the object area metric (OAM) measures $\mathrm{Prec}_{\mathrm{OAM}}$, $\mathrm{Sens}_{\mathrm{OAM}}$, $\mathrm{Spec}_{\mathrm{OAM}}$, and $\text{F-Score}_{\mathrm{OAM}}$.

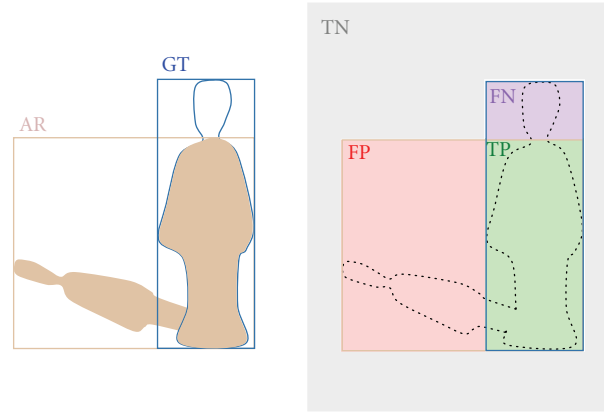


Figure 10: The difference in evaluating pixel accurate or using object bounding boxes. Left: pixel accurate GT and AR and their bounding boxes. Right: bounding box-based true positives (TPs), false positives (FPs), true negatives (TNs), and false negatives (FNs) are only an approximation of the pixel accurate areas.

*Precision ($\mathrm{Prec}_{OAM}$)*

Measures the false positive (*FP*) pixels which belong to the bounding boxes of the *AR* but not to the *GT*

$$\mathrm{Prec}_{\mathrm{OAM}} = \frac{\#\mathrm{TP}_p}{\#\mathrm{TP}_p + \#\mathrm{FP}_p}. \tag{22}$$

*Sensitivity ($\mathrm{Sens}_{OAM}$)*

Evaluates false negative *FN* pixels which belong to the bounding boxes of the *GT* but not to the *AR*:

$$\mathrm{Sens}_{\mathrm{OAM}} = \frac{\#\mathrm{TP}_p}{\#\mathrm{TP}_p + \#\mathrm{FN}_p}. \tag{23}$$

*Specificity ($Spec_{OAM}$)*

Considers true negative ($TN$) pixels, which neither belong to the $AR$ nor to the $GT$ bounding boxes:

$$\mathrm{Spec}_{\mathrm{OAM}} = \frac{\#\mathrm{TN}_p}{N}. \tag{24}$$

$N$ is the number of pixels in the image.

*F-Score ($F\text{-}Score_{OAM}$)*

Summarizes sensitivity and precision:

$$\text{F-Score}_{\mathrm{OAM}} = \frac{2 \cdot \mathrm{Prec}_{\mathrm{seg}} \cdot \mathrm{Sens}_{\mathrm{seg}}}{\mathrm{Prec}_{\mathrm{seg}} + \mathrm{Sens}_{\mathrm{seg}}}. \tag{25}$$

Further measures can be generated by comparing the spatial, temporal, or spatiotemporal accuracy between the observed and ground truth segmentation [35]. Measures for the spatial accuracy comprise shape fidelity, geometrical similarity, edge content similarity and statistical data similarity [35], negative rate metric, misclassification penalty metric, rate of misclassification metric, and weighted quality measure metric [13].

*Shape fidelity*

Is computed by the number of misclassified pixels of the $AR$ object and their distances to the border of the $GT$ object.

*Geometrical similarity [35]*

Measures similarities of geometrical attributes between the segmented objects. These include size (GSS), position (GSP), elongation (GSE), compactness (GSC), and a combination of elongation and compactness (GSEC):

$$\begin{aligned}
\mathrm{GSS} &= \left|\mathrm{area}(\mathrm{GT}) - \mathrm{area}(\mathrm{AR})\right|,\\
\mathrm{GSP} &= \left[\left(\mathrm{grav}_X\left(\left|\mathrm{area}(\mathrm{GT}) - \mathrm{grav}_X(\mathrm{AR})\right|\right)\right)^2\right.\\
&\quad \left. - \left(\mathrm{grav}_Y\left(\left|\mathrm{area}(\mathrm{GT}) - \mathrm{grav}_Y(\mathrm{AR})\right|\right)\right)^2\right]^{1/2},\\
\mathrm{GSE}(O) &= \frac{\mathrm{area}(O)}{\left(2 \times \mathrm{thickness}(O)\right)^2},\\
\mathrm{GSC}(O) &= \frac{\mathrm{perimeter}^2(O)}{\mathrm{area}(O)},\\
\mathrm{GSEC} &= \left|\frac{\mathrm{GSE}(\mathrm{GT}) - \mathrm{GSE}(\mathrm{AR})}{10} + \frac{\mathrm{GSC}(\mathrm{GT}) - \mathrm{GSC}(\mathrm{AR})}{150}\right|,
\end{aligned} \tag{26}$$

where area represents the segmented area of the objects, $\mathrm{grav}_X(O)$ and $\mathrm{grav}_Y(O)$are the center coordinates of the gravity of an object $O$, and thickness($O$)is the number of morphological erosion steps until an object disappears.

*Edge content similarity (ECS) [35]*

Yields a similarity based on edge content

$$\mathrm{ECS} = \mathrm{avg}(|\mathrm{Sobel}(\mathrm{GT} - \mathrm{AR})|) \tag{27}$$

with avg as average value and Sobel the result of edge detection by a Sobel filter.

*Statistical data similarity [35]*

Measures distinct statistical properties using brightness and redness (SDS)

$$\begin{aligned}
\mathrm{SDS} = \frac{3}{4 \times 255} &\left|\mathrm{avg}Y(\mathrm{GT}) - \mathrm{avg}Y(\mathrm{AR})\right|\\
&+ \left|\mathrm{avg}V(\mathrm{GT}) - \mathrm{avg}V(\mathrm{AR})\right|.
\end{aligned} \tag{28}$$

Here, avg$Y$ and avg$V$ are average values calculated in the YUV color model.

*Negative rate (NR) metric [13]*

Measures a false negative rate $\mathrm{NR}_{\mathrm{FN}}$ and false positive rate $\mathrm{NR}_{\mathrm{FP}}$ between matches of ground truth $GT$ and result $AR$ on a pixel-wise basis. The negative rate metric uses the number of false negative $\#\mathrm{FN}_p$ and false positive pixels $\#\mathrm{FP}_p$ and is defined via the arithmetic mean in contrast to the harmonic mean used in the $\text{F-Score}_{\mathrm{seg}}$:

$$\begin{aligned}
\mathrm{NR} &= \frac{1}{2}\left(\mathrm{NR}_{\mathrm{FN}} + \mathrm{NR}_{\mathrm{FP}}\right),\\
\mathrm{NR}_{\mathrm{FN}} &= \frac{\#\mathrm{FN}_p}{\#\mathrm{TP}_p + \#\mathrm{FN}_p},\\
\mathrm{NR}_{\mathrm{FP}} &= \frac{\#\mathrm{FP}_p}{\#\mathrm{TN}_p + \#\mathrm{FP}_p}.
\end{aligned} \tag{29}$$

*Misclassification penalty metric (MPM) [13]*

Values misclassified pixels by their distances from the $GT$ object border

$$\begin{aligned}
\mathrm{MPM} &= \frac{1}{2}\left(\mathrm{MPM}_{\mathrm{FN}} + \mathrm{MPM}_{\mathrm{FP}}\right),\\
\mathrm{MPM}_{\mathrm{FN}} &= \frac{1}{D}\sum_{k=1}^{\#\mathrm{FN}_p} d_{\mathrm{FN}}(k),\\
\mathrm{MPM}_{\mathrm{FP}} &= \frac{1}{D}\sum_{k=1}^{\#\mathrm{FP}_p} d_{\mathrm{FP}}(k),
\end{aligned} \tag{30}$$

where $d_{\mathrm{FN/FP}}(k)$ is the distance of the $k$th false negative/false positive pixel from the $GT$ object border, and $D$ is a normalization factor computed from the sum over all distances between $FP$ and $FN$ pixels and the object border.

*Rate of misclassification metric (RMM) [13]*

Describes the false segmented pixels by the distance to the border of the object in pixel units

$$\begin{aligned}
\mathrm{RMM} &= \frac{1}{2}\left(\mathrm{RMM}_{\mathrm{FN}} + \mathrm{RMM}_{\mathrm{FP}}\right),\\
\mathrm{RMM}_{\mathrm{FN}} &= \frac{1}{\#\mathrm{FN}_p}\sum_{k=1}^{\#\mathrm{FN}_p} \frac{d_{\mathrm{FN}}(k)}{D_{\mathrm{diag}}},\\
\mathrm{RMM}_{\mathrm{FP}} &= \frac{1}{\#\mathrm{FP}_p}\sum_{k=1}^{\#\mathrm{FP}_p} \frac{d_{\mathrm{FP}}(k)}{D_{\mathrm{diag}}},
\end{aligned} \tag{31}$$

where $D_{\mathrm{diag}}$ is the diagonal distance of the considered frame.

*Weighted quality measure metric (WQM) [13]*

Evaluates the spatial difference between $GT$ and $AR$ by the sum of weighted effects of false positive and false negative segmented pixels

$$\begin{aligned}
\mathrm{WQM} &= \ln\left(\frac{1}{2}\left(\mathrm{WQM}_{\mathrm{FN}} + \mathrm{WQM}_{\mathrm{FP}}\right)\right),\\
\mathrm{WQM}_{\mathrm{FN}} &= \frac{1}{\#\mathrm{FN}_p}\sum_{k=1}^{\#\mathrm{FN}_p} w_{\mathrm{FN}}\left(d_{\mathrm{FN}}(k)\right) d_{\mathrm{FN}}(k),\\
\mathrm{WQM}_{\mathrm{FP}} &= \frac{1}{\#\mathrm{FP}_p}\sum_{k=1}^{\#\mathrm{FP}_p} w_{\mathrm{FP}}\left(d_{\mathrm{FP}}(k)\right) d_{\mathrm{FP}}(k),\\
w_{\mathrm{FP}}(d_{\mathrm{FP}}) &= B_1 + \frac{B_2}{d_{\mathrm{FP}} + B_3}, \qquad w_{\mathrm{FN}}(d_{\mathrm{FN}}) = C\cdot d_{\mathrm{FN}}.
\end{aligned} \tag{32}$$

The constants were proposed as $B_1 = 19$, $B_2 = 178.125$, $B_3 = 9.375$, and $C = 2$ [13].

Temporal accuracy takes video sequences into consideration and assesses the motion of segmented objects. Temporal and spatiotemporal measures are often used in video surveillance, for example, misclassification penalty, shape penalty, and motion penalty [17].

*Misclassification penalty ($MP_{pix}$) [17]*

Penalizes the misclassified pixels that are farther from the $GT$ more heavily:

$$\mathrm{MP}_{\mathrm{pix}} = \frac{\sum_{x,y} I(x,y,t)\mathrm{cham}(x,y,t)}{\sum_{x,y}\mathrm{cham}(x,y,t)}, \tag{33}$$

where $I(x, y, t)$ is an indicator function with value 1 if $AR$ and $GT$ are different, and cham denotes the chamfer distance transform of the boundary of $GT$.

*Shape penalty ($MP_{shape}$) [17]*

Considers the turning angle function of the segmented boundaries:

$$\mathrm{MP}_{\mathrm{shape}} = \frac{\sum_{k=1}^{K}\left|\Theta^t_{\mathrm{GT}}(k) - \Theta^t_{\mathrm{AR}}(k)\right|}{2\pi K}, \tag{34}$$

and $\Theta^t_{\mathrm{GT}}(k)$, $\Theta^t_{\mathrm{AR}}(k)$ denote the turning angle function of the $GT$ and $AR$, and $K$ is the total number of points in the turning angle function.

*Motion penalty ($MP_{mot}$) [17]*

Uses the motion vectors $\vec{v}\,(t)$ of $GT$ and $AR$ objects

$$\mathrm{MP}_{\mathrm{mot}} = \frac{\left|\left|\vec{v}_{\mathrm{GT}}(t) - \vec{v}_{\mathrm{AR}}(t)\right|\right|}{\left|\left|\vec{v}_{\mathrm{GT}}(t)\right|\right| + \left|\left|\vec{v}_{\mathrm{AR}}(t)\right|\right|}. \tag{35}$$

Nghiem et al. [16, 34] propose further segmentation measures adapted to the video surveillance application. These measures take into account how well a segmentation method performs in special cases such as appearance of shadows (shadow contrast levels) and handling of split and merge situations (split metric and merge metric).

#### 4.3.1. Chosen segmentation measure subset

Due to the enormous costs and expenditure of time to generate pixel-accurate segmentation ground truth, we decided to be content with an approximation of the real segmentation data. This approximation is given by the already labeled bounding boxes and enables us to apply our segmentation metric to a huge number of sequences, which makes it easier to get more representative results. The metrics we chose is equal to the above mentioned object area metric proposed in [15]:

(i) $\mathrm{Prec}_{\mathrm{OAM}}$ (22),

(ii) $\mathrm{Sens}_{\mathrm{OAM}}$ (23),

(iii) $\text{F-Score}_{\mathrm{OAM}}$ (25).

The benefit of this metric is its independence from assignments between $GT$ and $AR$ objects as described in Section 4.2. Limitations are given by inexactness due to the discrepancy between the areas of the objects and their bounding boxes as well as the inability to take into account the areas of occluded objects.

### 4.4. Object detection measures

In order to get meaningful values that represent the ability of the system to fulfill the object detection tasks, the numbers of correctly detected, falsely detected, or misdetected objects are merged into appropriate formulas to calculate detection measures like detection rates or precision and sensitivity. Proposals for object detection metrics mostly concur in their use of formulas, however the definition of a good detection of an object differs.

#### 4.4.1. Object-counting approach

The simplest way to calculate detection measures is to compare the $AR$ objects to the $GT$ object according only to their presence whilst disregarding their position and size.

*Configuration distance (CD) [33]*

Smith et al. [33] present the configuration distance, which measures the difference between the number of $GT$ and $AR$ objects and is normalized by the instantaneous number of $GT$ objects in the given frame

$$\mathrm{CD} = \frac{\#\mathrm{AR}_o - \#\mathrm{GT}_o}{\max\left(\#\mathrm{GT}_o, 1\right)}, \tag{36}$$

where $\#\mathrm{AR}_o$ is the number of $AR$ objects and $\#\mathrm{GT}_o$ the number of $GT$ objects in the current frame. The result is zero if $\#\mathrm{GT}_o = \#\mathrm{AR}_o$, negative when $\#\mathrm{GT}_o > \#\mathrm{AR}_o$, and positive when $\#\mathrm{GT}_o < \#\mathrm{AR}_o$, which gives an indication of the direction of the failure.

*Number of objects [15]*

The collection of the metrics evaluated by [15] contains a metric only concerning the number of objects, consisting of a precision and a sensitivity value

$$\begin{aligned} \text{Prec}_{\text{NO}} &= \frac{\min\left(\#\text{AR}_o, \#\text{GT}_o\right)}{\#\text{AR}_o}, \\ \text{Sens}_{\text{NO}} &= \frac{\min\left(\#\text{AR}_o, \#\text{GT}_o\right)}{\#\text{GT}_o}. \end{aligned} \tag{37}$$

The global values are computed by averaging the frame-wise values taking into account only frames containing at least one object. Further information about averaging can be found in Section 4.11.

The drawback of the approaches based only on counting objects is that multiple failures could compensate and result in an apparently perfect values for these measures. Due to the limited significance of measures based only on object counts, most approaches for detection performance evaluation contain metrics taking into account the matching of *GT* and *AR* objects.

### 4.4.2. Object-matching approach

Object matching based on centroids as well as on the object area overlap is described in detail in Section 4.2. Though the matching based on object centroids is a quick and easy way to assign *GT* and *AR* objects, it does not provide reliable assignments in complex situations (Section 4.2.1). Since the matching based on the object area overlap does not feature these drawbacks (Section 4.2.2), we decided to determine object correspondences via the overlap and to add this metric to our environment. After the assignment step, precision and sensitivity are calculated according to ETISEO metric M1.2.1 [15]. This corresponds to the following measures which we added to our environment:

$$\text{Prec}_{\text{det}} = \frac{\#\text{TP}_o}{\#\text{TP}_o + \#\text{FP}_o}, \tag{38}$$

$$\text{Sens}_{\text{det}} = \frac{\#\text{TP}_o}{\#\text{TP}_o + \#\text{FN}_o}, \tag{39}$$

$$\text{F-Score}_{\text{det}} = \frac{2 \cdot \text{Prec}_{\text{det}} \cdot \text{Sens}_{\text{det}}}{\text{Prec}_{\text{det}} + \text{Sens}_{\text{det}}}. \tag{40}$$

The averaged metrics for a sequence are computed as the sum of the values per frame divided by the number of frames containing at least one *GT* object. Identical to the segmentation measure, we use the harmonic mean of precision and sensitivity for evaluating the balance between these aspects.

The fact that only one-to-one correspondences are allowed results in the deterioration of this metric in merge situations. Thus, it can be used to test the capabilities of the system to separately detect single objects, which is of major importance in cases of groups of objects or occlusions.

The property mentioned above makes this metric only partly appropriate to evaluate the detection capabilities of a system independently from the real number of objects in segmented blobs. In test sequences where single persons are merged into groups, for example, this metric gives the illusion that something was missed, though there was just no separation of groups of persons into single objects.

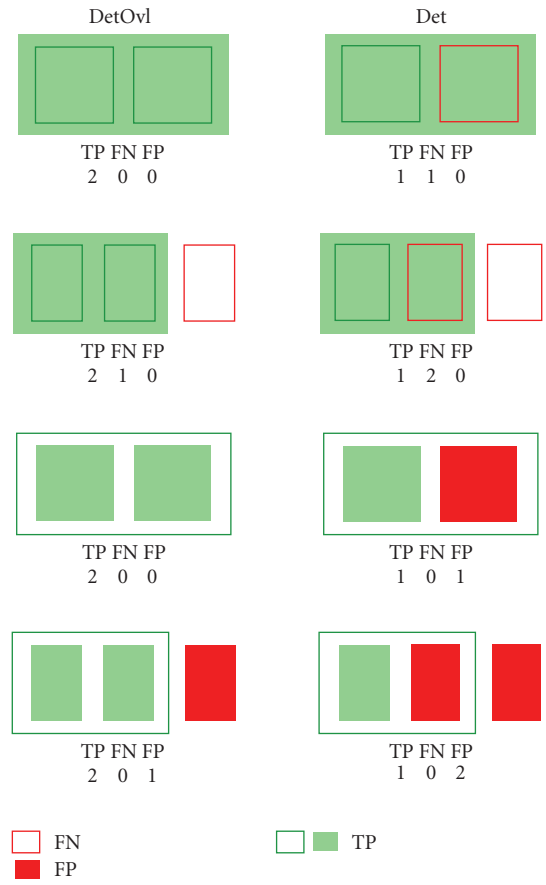


Figure 11: Comparison of strict and lenient detection measures.

In addition to the strict metric, we use a lenient metric allowing multiple assignments and being content with a minimal overlap. Calculation proceeds in the same manner as for the strict metric, except that due to the modified method of assignment, the deviating definitions of *TP*, *FP*, and *FN* result in these new measures.

(i) $\text{Prec}_{\text{detOvl}}$,

(ii) $\text{Sens}_{\text{detOvl}}$,

(iii) $\text{F-Score}_{\text{detOvl}}$.

Figure 11 exemplifies the difference between the strict and the lenient metric applied to two combinations for the split and the merge case. The effects of the strict assignment can be seen in the second column where each object is assigned to only one corresponding object, and all the others are treated as false detections, although they have passed the distance criterion. The consequences in the merge case are more *FN*s and in the split case more *FP*s.

There are metrics directly addressing the split and merge behavior of the algorithm. In the split case, the number of *AR* objects which can be assigned to a *GT* object is counted and

in the case of a merge, it is determined how many *GT* objects correspond to an *AR* object. This is in accordance with the ETISEO metrics M2.2.1 and M2.3.1 [15]. The definition of the ETISEO metric M2.2.1 is

$$\text{Split} = \frac{1}{\#\text{GT}_f} \cdot \sum_{\text{GT}_f} \left( \frac{1}{\#\text{GT}_o} \sum_{l=1}^{\#\text{GT}_o} \frac{1}{\#(\text{AR}_o \longrightarrow \text{GT}_o(l))} \right), \quad (41)$$

where $\#(\text{AR}_o \rightarrow \text{GT}_o(l))$ is the number of *AR* objects for which the matching criteria allow an assignment to the corresponding *GT* objects and $\#\text{GT}_f$ is the number of frames which contain at least one *GT* object. For every frame, the average inverse over all *GT* objects is computed. The value for the whole sequence is then determined by summing the values of every frame and dividing by the number of frames in which at least one *GT* object occurs.

For this measure, the way of assigning the objects is of paramount importance. When objects fragment into several smaller objects, the single fragments often do not meet the matching criteria used for the detection measures. Therefore, a matching criterion that allows to assign *AR* objects which are much smaller then the corresponding *GT* objects needs to be used. For the ETISEO benchmarking [6], the distance measure D5-overlapping [15] was used as it satisfies this requirement.

Another problem is that in the case of complex scenes with occlusions, fragments of one *AR* object should not be assigned to several *GT* objects simultaneously as this would falsely worsen the value of this measure. Each *AR* object which represents a fragment should only be allowed to be counted once. Therefore, the following split measure is integrated in the presented ATE:

*Split resistance (SR)*

$$\text{SR} = \frac{1}{\#\text{GT}_o} \cdot \sum_{l=1}^{\#\text{GT}_o} \frac{1}{1 + \#\text{add. split fragments } (l)}, \qquad \text{SR}_{\text{AvM}} = \frac{1}{\#\text{GT}_f} \cdot \sum_{\text{GT}_f} \text{SR}. \quad (42)$$

The assignment criteria used here are constructed to allow minimal overlaps to lead to an assignment, thus avoiding the overlooking of fragments.

The corresponding metric for the merge case presented by ETISEO M2.3.1 [15] is

$$\text{Merge} = \frac{1}{\#\text{GT}_f} \cdot \sum_{\text{GT}_f} \left( \frac{1}{\#\text{AR}_o} \sum_{l=1}^{\#\text{AR}_o} \frac{1}{\#(\text{GT}_o \longrightarrow \text{AR}_o(l))} \right), \quad (43)$$

where $\#(\text{GT}_o \rightarrow \text{AR}_o(l))$ is the number of *GT* objects which can be assigned to the corresponding *AR* objects due to the matching criterion used.

For the merge case, the same problems concerning the assignment must be addressed as for the split case. Thus, the proposed metric for the merge case is

*Merge resistance (MR)*

$$\text{MR} = \frac{1}{\#\text{AR}_o} \sum_{l=0}^{\#\text{AR}_o} \frac{1}{1 + \#\text{add. merged objects } (l)}, \qquad \text{MR}_{\text{AvM}} = \frac{1}{\#\text{AR}_f} \sum_{\text{AR}_f} \text{MR}. \quad (44)$$

The classification if there is a split or merge situation can also be achieved by storing matches between *GT* and *AR* objects in a matrix and then analyzing its elements and sums over columns and rows [37]. A similar approach is described by Smith et al. [33], which use configuration maps containing the associations between *GT* and *AR* objects to identify and count configuration errors like false positives, false negatives, merging and splitting. An association between a *GT* and an *AR* object is given if they pass the coverage test, that is, the matching value exceeds the applied threshold. To infer *FP*s and merging, a configuration map from the perspective of the *AR*s is inspected, and *FN*s and splitting are identified by a configuration map from the perspective of the *GT*s. Multiple entries indicate merging, respectively, splitting and blank entries indicate *FP*s, respectively, *FN*s.

#### 4.4.3. Chosen object detection measure subset

To summarize the section above, these are the object detection measures used in our ATE.

(i) Detection performance (strict assignment):
  (a) $\text{Prec}_{\text{det}}$ (38),
  (b) $\text{Sens}_{\text{det}}$ (39),
  (c) $\text{F-Score}_{\text{det}}$ (40).

(ii) Detection performance (lenient assignment):
  (a) $\text{Prec}_{\text{detOvl}}$,
  (b) $\text{Sens}_{\text{detOvl}}$,
  (c) $\text{F-Score}_{\text{detOvl}}$.

(iii) Merge resistance:
  (a) MR (44).

(iv) Split resistance:
  (a) SR (42).

In addition, we use a normalized measure for the rate of correctly detected alarm situations, where an alarm situation is a frame containing at least one object of interest.

*Alarm correctness rate (ACR)*

The number of correctly detected alarm and nonalarm situations in relation to the number of frames:

$$\text{ACR} = \frac{\#\text{TP}_f + \#\text{TN}_f}{\#\text{frames}}. \quad (45)$$

### 4.5. Object localization measures

The metrics above give insight into the system's capability of detecting objects. However, they do not provide information of how precisely objects have been detected. In other words, how precisely region and position of the assigned *AR* match the *GT* bounding boxes.

This requires certain metrics expressing the precision numerically. The distance of the centroids discussed in Section 4.2.1 is one possibility, which requires normalization to keep the desired range of values. The problem lies in this very fact, since finding a normalization which does not deteriorating the metric's relevance is difficult. The following section introduces our experiment and finally explains why we are not completely satisfied with its results. In order to make 0 the worst, and 1 the best value, we have to transform the Euclidean distance used in the distance definitions of the object centroid matching into a matching measure by subtracting the normalized distance from 1. Normalization commences along the larger of the two bounding box's diagonals. This results in the following object localization measure definitions for each pair of objects:

*Relative object centroid distance (ROCD)*

$$\mathrm{ROCD} = \frac{\sqrt{(x_{\mathrm{GT}} - x_{\mathrm{AR}})^2 + (y_{\mathrm{GT}} - y_{\mathrm{AR}})^2}}{\max(d_{\mathrm{GT}}, d_{\mathrm{AR}})}, \tag{46}$$

*Relative object centroid match (ROCM)*

$$\mathrm{ROCM} = 1 - \mathrm{ROCD}. \tag{47}$$

In theory, the worst value 0 is reached as soon as the centroid's distance equals or exceeds the larger bounding box's diagonal. In fact, this case will not come about, since these *AR*/*GT* combinations of the above-described matching criteria are not meant to occur in the first place. Their bounding boxes do not overlap anymore here. Unfortunately, this generous normalization results in merely exploiting only the upper possible range of values, and in only a minor deviation between the best and worst value for this metric. In addition, significant changes in detection precision are represented only by moderate changes of the measure. Another drawback is at hand. When an algorithm tends to oversegment objects, it will have a positive impact on the value of ROCM, lowering its relevance.

A similar problem occurs when introducing a metric for evaluating the size of *AR* bounding boxes. One way to resolve this would be to normalize the absolute region difference [14], another would be using a ratio of *AR* and *GT* bounding boxes' regions. We added the metric relative object area match (ROAM) to our ATE, which represents the discrepancy of the sizes of *AR* and *GT* bounding boxes. The ratio is computed by dividing the smaller by the larger size, in order to not exceed the given range of value, that is,

*Relative object area match (ROAM)*

$$\mathrm{ROAM} = \frac{\min(A_{\mathrm{GT}}, A_{\mathrm{AR}})}{\max(A_{\mathrm{GT}}, A_{\mathrm{AR}})}. \tag{48}$$

Information about the *AR* bounding boxes being too large or too small compared to the *GT* bounding boxes is lost in the process.

Still missing is a metric representing the precision of the detected objects. Possible metrics were presented with $\mathrm{Prec}_{\mathrm{OAM}}$, $\mathrm{Sens}_{\mathrm{OAM}}$, and $\text{F-Score}_{\mathrm{OAM}}$ in Section 4.3. Instead of globally using this metric, we apply them to certain pairs of *GT* and *AR* objects (in parallel to [33]) measuring the object area coverage. For each pair, this results in values for $\mathrm{Prec}_{\mathrm{OAC}}$, $\mathrm{Sens}_{\mathrm{OAC}}$, and $\text{F-Score}_{\mathrm{OAC}}$. As mentioned above, $\text{F-Score}_{\mathrm{OAC}}$ is identical to the computed dice coefficient (21).

The provided equations of the three different metrics that evaluate the matching of *GT* and *AR* bounding boxes relate to one pair in each case. In order to have one value for each frame, the values, resulting in the object correspondences, are averaged. The global value for a whole sequence is the average value over all frames featuring at least one object correspondence.

Unfortunately, averaging raises dependencies to the detection rate, which can lead to distortion of results when comparing different algorithms. The problem lies in the fact that only values of existing assignments have an impact on the average value. If a system is parameterized to be insensitive, it will detect only very few objects but these precisely. Such a system will achieve much better results than a system detecting all *GT* objects but not matching them precisely.

Consequently, these metrics should not be evaluated separately, but always together with the detection measures. The more the values of the detection measures differ, the more questionable the values of the localization measures become.

#### 4.5.1. Chosen object localization measure subset

Here is a summarization of the object localization measures chosen by us:

(i) relative object centroid match:

  (a) ROCM (47),

(ii) relative object area match:

  (a) ROAM (48),

(iii) object area coverage:

  (a) $\mathrm{Prec}_{\mathrm{OAC}}$,
  (b) $\mathrm{Sens}_{\mathrm{OAC}}$,
  (c) $\text{F-Score}_{\mathrm{OAC}}$.

### 4.6. Tracking measures

Tracking measures apply over the lifetime of single objects, which are called tracks. In contrast to detection measures,

which evaluate the detection rate of anonymous objects for every single frame, tracking measures compute the ability of a system to track objects over time. The discrimination between different objects is usually done via an unique ID for every object. The tracking measures for one sequence are thus not computed via an averaging of frame-based values, but rather by using averaging over the frame-wise values of the single tracks. The first step consists therefore of the assignment of *AR* to *GT* tracks. Two different approaches can be found for this task.

#### 4.6.1. Track assignment based on trajectory matching

Senior et al. [10] match the trajectories. For this purpose, they compute for every *AR* and *GT* track combination a distance value which is defined as follows:

$$D_{\mathrm{AR,GT}}(i_1,i_2) = \frac{1}{N_{\mathrm{AR,GT}}(i_1,i_2)} \times \sum_j \Big( |\vec{x}_{\mathrm{AR}}(i_1,j) - \vec{x}_{\mathrm{GT}}(i_2,j)|^2 + |\vec{v}_{\mathrm{AR}}(i_1,j) - \vec{v}_{\mathrm{GT}}(i_2,j)|^2 + |\vec{s}_{\mathrm{AR}}(i_1,j) - \vec{s}_{\mathrm{GT}}(i_2,j)|^2 \Big)^{1/2}, \tag{49}$$

where $N_{\mathrm{AR,GT}}(i_1,i_2)$ is the number of points in both tracks $\mathrm{AR}_{\mathrm{tr}}(i_1)$ and $\mathrm{GT}_{\mathrm{tr}}(i_2)$, $\vec{x}_{\mathrm{AR}}(i_1,j)$ or $\vec{x}_{\mathrm{GT}}(i_2,j)$ is the centroid of the bounding box of an *AR* or *GT* track at frame $j$, $\vec{v}_{\mathrm{AR}}(i_1,j)$ or $\vec{v}_{\mathrm{GT}}(i_2,j)$ is the velocity and $\vec{s}_{\mathrm{AR}}(i_1,j)$ or $\vec{s}_{\mathrm{GT}}(i_2,j)$ is the vector of width and height of track $i_1$ or $i_2$ at frame $j$.

This way of comparing trajectories, which takes the position, the velocities, and the objects' bounding boxes into account, is also used in a reduced version of (49) in [11, 14, 30] considering only the position of the object:

$$D_{\mathrm{AR,GT}}(i_1,i_2) = \frac{1}{N_{\mathrm{AR,GT}}(i_1,i_2)} \sum_j |\vec{x}_{\mathrm{AR}}(i_1,j) - \vec{x}_{\mathrm{GT}}(i_2,j)|. \tag{50}$$

The calculation of the distance matrix according to (50) is included in Figure 12 and marked as *Step 2*. *Step 1* represents the analysis of temporal correspondence and hence the calculation of the number of overlapping frames. In order to actually establish the correspondence between *AR* and *GT* tracks, a thresholding step (*Step 3* in Figure 12) has to be applied. The resulting track correspondence is represented by a binary mask, which is simply calculated by assigning a *one* to those matrix elements which exceed a given threshold and *zero* in the alternative case.

Track correspondence is established by thresholding this matrix. Each track in the ground truth can be assigned to one or more tracks from the results. This accommodates fragmented tracks. Once the correspondence between the ground truth and the result tracks is established, the following error measures are computed between the corresponding tracks:

*False positive track error rate ($\mathrm{TER}_{FP}$)*

$$\mathrm{TER}_{\mathrm{FP}} = \frac{\#\mathrm{AR}_{\mathrm{tr}} - \#(\mathrm{AR}_{\mathrm{tr}} \longrightarrow \mathrm{GT}_{\mathrm{tr}})}{\#\mathrm{GT}_{\mathrm{tr}}}, \tag{51}$$

*False negative track error rate ($\mathrm{TER}_{FN}$)*

$$\mathrm{TER}_{\mathrm{FN}} = \frac{\#\mathrm{AR}_{\mathrm{tr}} - \#(\mathrm{GT}_{\mathrm{tr}} \longrightarrow \mathrm{AR}_{\mathrm{tr}})}{\#\mathrm{GT}_{\mathrm{tr}}}. \tag{52}$$

*Object detection lag*

This is the time difference between the ground truth identifying a new object and the tracking algorithm detecting it. Time-shifts between tracks and an evaluation of (spatio-)temporally separated *GT* and *AR* tracks using statistics are discussed in more detail by [38].

If an *AR* track is assigned to a *GT* track, metrics are needed to assess the quality of the representation by the *AR* track. One criterion for that is the temporal overlap, respectively, the temporal incongruity as rated in the following metric.

*Track incompleteness factor (TIF)*

$$\mathrm{TIF} = \frac{\#\mathrm{FN}_f(i) + \#\mathrm{FP}_f(i)}{\#\mathrm{TP}_f(i)}, \tag{53}$$

where $\mathrm{FN}_f(i)$ is the false negative frame count, that is, the number of frames that are missing from the *AR* Track, $\mathrm{FP}_f(i)$ is the false positive frame count, that is, the number of frames that are reported in the *AR* which are not present in the *GT*, and $\mathrm{TP}_f(i)$ is the number of frames present in both *AR* and *GT*.

Once not only the presence but also the the correspondence between the ground truth and the result tracks is established according to the trajectory matching, the following error measures are computed between the corresponding tracks.

*Track detection rate (TDR)*

The track detection rate indicates the tracking completeness of a specific ground truth track. The measure is calculated as follows

$$\mathrm{TDR} = \frac{\#\mathrm{TP}_f(i)}{\#\text{frames } \mathrm{GT}_{\mathrm{tr}}(i)}, \tag{54}$$

where $\#\text{frames } \mathrm{GT}_{\mathrm{tr}}(i)$ is the number of the frames of the $i$th *GT* track. In [11], $\#\mathrm{TP}_f(i)$ is defined as the number of frames of the $i$th *GT* track that correspond to an *AR* track.

*Tracker detection rate (TRDR)*

This measure characterizes the tracking performance of the object tracking algorithm. It is basically similar to the TDR measure, but considers entities larger than just single tracks

$$\mathrm{TRDR} = \frac{\sum_i \#\mathrm{TP}_f(i)}{\sum_i \#\text{frames } \mathrm{GT}_{\mathrm{tr}}(i)}, \tag{55}$$

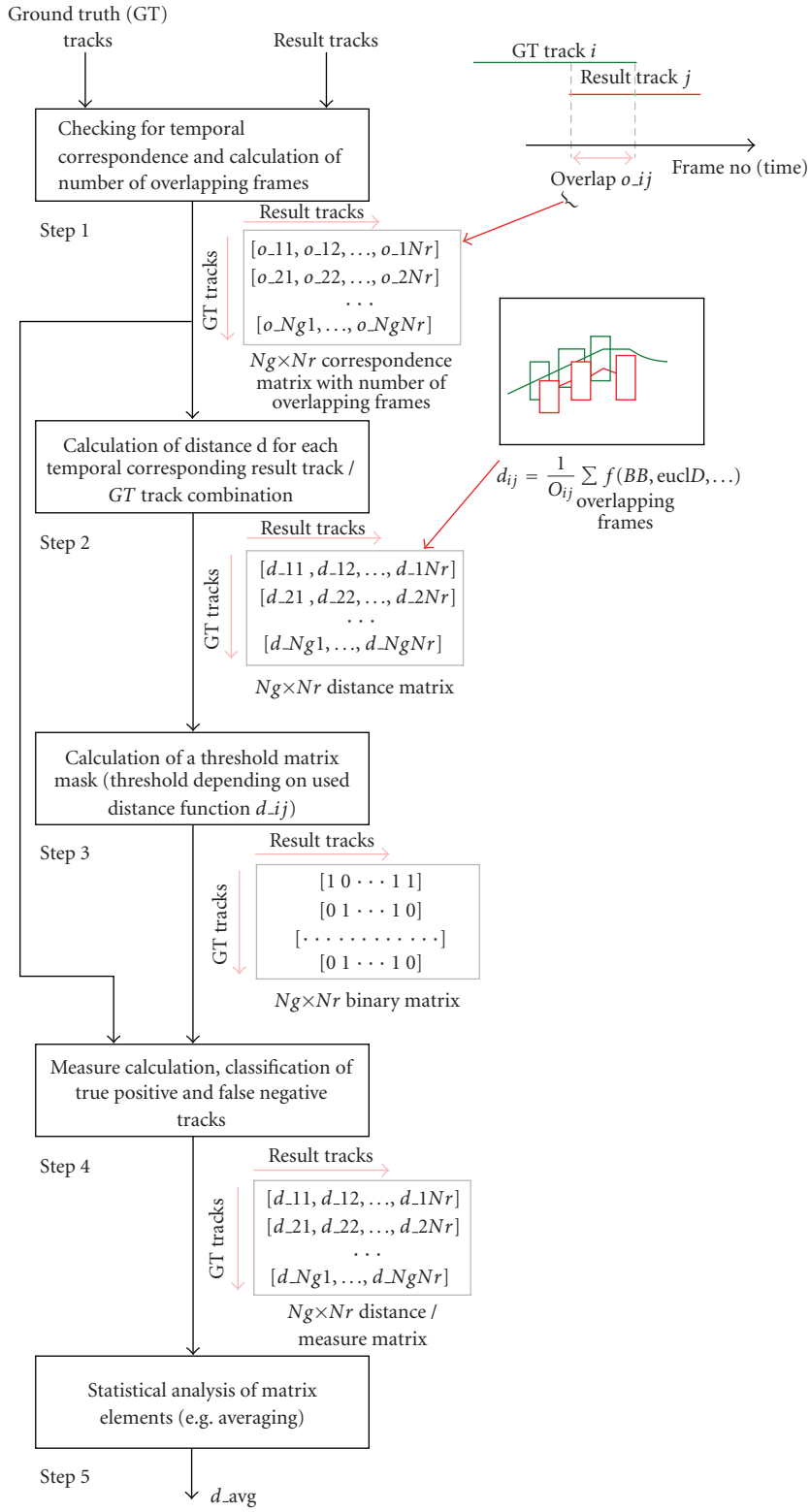


Figure 12: Overview of the measure calculation procedure as applied in [14]. *Step 1* represents the analysis of temporal correspondence and hence the calculation of the number of overlapping frames. The calculation of the distance matrix according to (50) is performed in *Step 2*. In order to actually establish the correspondence between *AR* and *GT* tracks, a thresholding step has to be applied (*Step 3*). The resulting track correspondence is represented by a binary mask, which is simply calculated by assigning a *one* to those matrix elements which exceed a given threshold and *zero* in the alternative case. In *Step 4*, the actual measures are computed. Further, additional analysis is performed in *Step 5*.

where #frames $\mathrm{GT}_{\mathrm{tr}}(i)$ is the number of the frames of the $i$th $GT$ track.

*False alarm rate (FAR)*

The FAR measures also the tracking performance of the object tracking algorithm. It is defined as follows

$$\mathrm{FAR} = \frac{\sum_i \#\mathrm{FP}_f(i)}{\sum_i \#\text{frames } \mathrm{AR}_{\mathrm{tr}}(i)}, \tag{56}$$

where #frames $\mathrm{AR}_{\mathrm{tr}}(i)$ is the number of the frames of the $i$th $AR$ track. In [11], $\mathrm{FP}_f(i)$ is defined as one object of the $i$th $AR$ track, that is tracked by the system and does not have a matching ground truth point.

*Track fragmentation (TF)*

Number of result tracks matched to a ground truth track

$$\mathrm{TF} = \frac{1}{\#\mathrm{TP}_{\mathrm{GT}_{\mathrm{tr}}}} \sum_i \#(\mathrm{AR}_{\mathrm{tr}} \longrightarrow \mathrm{GT}_{\mathrm{tr}}(i)). \tag{57}$$

*Occlusion success rate (OSR)*

$$\mathrm{OSR} = \frac{\text{Number of successful dynamic occlusions}}{\text{Total number of dynamic occlusions}}. \tag{58}$$

*Tracking success rate (TSR)*

$$\mathrm{TSR} = \frac{\text{Number of non-fragmented tracked GT tracks}}{\#\mathrm{GT}_{\mathrm{tr}}}. \tag{59}$$

#### 4.6.2. Track assignment based on frame-wise object matching

The second approach to assign the $AR$ to the $GT$ tracks is to use the same frame-wise object correspondences as for the detection measures as mentioned in Section 4.4. However, those correspondences are not always correct. Ideally, each $GT$ track is matched by exactly one $AR$ track, though it does not necessary hold in practice. To associate identities properly it has been proposed that identification associations can be formed on a "majority rule" basis [33], where an $AR$ track is assigned to the $GT$ track with which it has the maximal corresponding time, and a $GT$ track is assigned to the $AR$ track which corresponds to it for the largest amount of time. Based on the definitions above, four tracking measures are introduced. Two of them measure the identification errors.

*Falsely identified tracker (FIT)*

An $AR$ track segment which passes the coverage test for a $GT$ track but is not the identifying $AR$ track for it (see Figure 13):

$$\overline{\mathrm{FIT}} = \frac{1}{\#\text{frames}} \sum_j \frac{\#\mathrm{FIT}(j)}{\max\left(\#\mathrm{GT}_{\mathrm{tr}}(i)(j), 1\right)}. \tag{60}$$

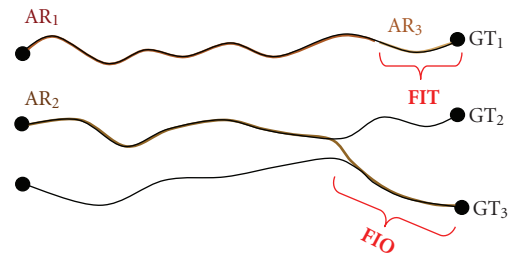


Figure 13: Example for identification errors proposed by [33]. Three $GT$ objects are tracked by three $AR$ objects. A falsely identified tracker error (FIT) occurs when $\mathrm{GT}_1$ is tracked by a second corresponding $AR$ track $\mathrm{AR}_3$. A falsely identified object error (FIO) occurs when an $AR$ track swaps the corresponding $GT$ track, here this is the case for $\mathrm{AR}_2$ swapping from $\mathrm{GT}_2$ to $\mathrm{GT}_3$. The time intervals where a FIT, respectively, FIO occur are marked.

*Falsely identified object (FIO)*

A $GT$ track segment which passes the coverage test for an $AR$ but is not the identifying $GT$ track (see Figure 13):

$$\overline{\mathrm{FIO}} = \frac{1}{\#\text{frames}} \sum_j \frac{\#\mathrm{FIO}(j)}{\max\left(\#\mathrm{GT}_{\mathrm{tr}}(j), 1\right)}. \tag{61}$$

The other two measures are similar to TDR and FAR but more strict, because they rate only correspondences with the identifying track as correct.

*Tracker purity (TPU)*

The tracker purity indicates the degree of consistency to which an $AR$ track identifies a $GT$ track

$$\mathrm{TPU} = \frac{\#\text{correct frames } \mathrm{AR}_{\mathrm{tr}}(i)}{\#\text{frames } \mathrm{AR}_{\mathrm{tr}}(i)}, \tag{62}$$

where $\#\mathrm{frames}_{\mathrm{AR}}(i)$ is the number of frames of the $i$th $AR$ track and $\#\text{correct frames}_{\mathrm{AR}}(i)$ the number of frames that the $i$th $AR$ track identifies a $GT$ track correctly.

*Object purity (OPU)*

The object purity indicates the degree of consistency to which a $GT$ track is identified by an $AR$ track:

$$\mathrm{OPU} = \frac{\#\text{correct frames } \mathrm{GT}_{\mathrm{tr}}(i)}{\#\text{frames } \mathrm{GT}_{\mathrm{tr}}(i)}, \tag{63}$$

where #frames $\mathrm{GT}_{\mathrm{tr}}(i)$ is the number of the frames of the $i$th $GT$ track and #correct frames $\mathrm{GT}_{\mathrm{tr}}(i)$ is the number of frames that the $i$th $GT$ track is identified by an $AR$ track correctly.

The ETISEO metrics [15] provide tracking measures which are similar to the above-mentioned ones. Metric M3.2.1 calculates a track-based $\mathrm{Prec}_{\mathrm{track}}$, $\mathrm{Sens}_{\mathrm{track}}$, and $\text{F-Score}_{\mathrm{track}}$. The $\mathrm{Sens}_{\mathrm{track}}$ conforms to (52), because $\mathrm{Sens}_{\mathrm{track}} = 1 - \mathrm{TER}_{\mathrm{FN}}$, but the $\mathrm{Prec}_{\mathrm{track}}$ differs from $1 - \mathrm{TER}_{\mathrm{FP}}$ (51), because it refers to the number of $AR$ tracks instead of the number of $GT$ tracks. Another metric in [15] is the

"tracking time" (M3.3.1), which is the same as the OPU above.

To assess the consistency of the object IDs, the metrics persistence (M3.4.1) and confusion (M3.5.1) are used.

*Persistence (Per)*

Evaluates the persistence of the ID

$$\mathrm{Per} = \frac{1}{\#\mathrm{GT_{tr}}} \sum_i \frac{1}{\#(\mathrm{AR_{tr}} \longrightarrow \mathrm{GT_{tr}}(i))}. \tag{64}$$

*Confusion (Conf)*

Indicates the robustness to confusion along the time

$$\mathrm{Conf} = \frac{1}{\#(\mathrm{GT_{tr}} \longrightarrow \mathrm{AR_{tr}})} \sum_i \frac{1}{\#(\mathrm{GT_{tr}} \longrightarrow \mathrm{AR_{tr}}(i))}, \tag{65}$$

where $\#(\mathrm{AR_{tr}} \rightarrow \mathrm{GT_{tr}}(i))$ indicates the number of *AR* tracks that correspond to the *i*th *GT* track and vice versa for $\#(\mathrm{GT_{tr}} \rightarrow \mathrm{AR_{tr}}(i))$.

### 4.6.3. Chosen tracking measure subset

For our evaluations, the assignment of tracks is done via frame-based correspondences as described in Section 4.6.2. Using that strategy, we compute the following measures.

*False positive track resistance ($\mathrm{TR_{FP}}$)*

Assesses the ability of the system to prevent *FP* tracks, which are *AR* tracks without any correspondence to a *GT* track:

$$\mathrm{TR_{FP}} = 1 - \frac{\#\mathrm{AR_{tr}} - \#(\mathrm{AR_{tr}} \longrightarrow \mathrm{GT_{tr}})}{\#\mathrm{AR_{tr}}}. \tag{66}$$

Note the division by $\#\mathrm{AR_{tr}}$ instead of $\#\mathrm{GT_{tr}}$ (compare to (51)).

*False negative track resistance (FNTR)*

Assesses the ability of the system to prevent *FN* tracks, which are *GT* tracks without any correspondence to an *AR* track

$$\mathrm{TR_{FN}} = 1 - \mathrm{TER_{FN}}. \tag{67}$$

*Track coverage rate (TCR)*

Measures how long an *AR* track has correspondences to *GT* tracks in relation to its lifetime

$$\mathrm{TCR} = \frac{\#\text{ass. frames } \mathrm{GT_{tr}}(i)}{\#\text{frames } \mathrm{GT_{tr}}(i)}, \tag{68}$$

where $\#\text{frames } \mathrm{GT_{tr}}(i)$ is the number of frames of the *i*th *GT* track and $\#\text{ass. frames } \mathrm{GT_{tr}}(i)$ is the number of frames that the *i*th *GT* track is identified by at least one *AR* track.

*Track fragmentation resistance (TFR)*

Assesses the ability to track an *GT* object without changing the ID of the *AR* track. The more *AR* tracks are assigned over the *GT* track's lifetime, the worse is the value of this metric:

$$\mathrm{TFR} = \frac{1}{\#\mathrm{TP_{GT_{tr}}}} \sum_i \frac{1}{\#(\mathrm{AR_{tr}} \longrightarrow \mathrm{GT_{tr}}(i))_{1:1}}, \tag{69}$$

where $\#(\mathrm{AR_{tr}} \rightarrow \mathrm{GT_{tr}}(i))_{1:1}$ indicates the number of *AR* tracks that correspond to the *i*th *GT* track. If there are multiple correspondences at the same time for one *GT* track, the best one is taken into account. *GT* tracks without correspondences ($\mathrm{FN_{tr}}$) are omitted.

*Tracking success rate (TSR)*

Analogue to (59). We also adopt the four tracking measures from [33] with partially small modifications.

*Tracker purity (TPU)*

Is identical to (62), but with $N_{\mathrm{AR}}$ as the number of *AR* tracks excluding *FP* tracks. Otherwise, the *FP* tracks would dominate this measure and the changes that this measure is established to assess would be occluded.

*Object purity (OP)*

Equal to (63).

To fulfill our normalization constraints, we transform the errors FIT and FIO into resistances.

*Falsely identified tracker resistance (FITR)*

$$\mathrm{FITR} = 1 - \frac{1}{\#\text{ass. frames}_{\mathrm{AR,GT}}} \sum_j \frac{\#\mathrm{FIT}(j)}{\max\left(\#\mathrm{GT_{tr}}(j), 1\right)}. \tag{70}$$

*Falsely identified object resistance (FIOR)*

$$\mathrm{FIOR} = 1 - \frac{1}{\#\text{ass. frames}_{\mathrm{AR,GT}}} \sum_j \frac{\#\mathrm{FIO}(j)}{\max\left(\#\mathrm{GT_{tr}}(j), 1\right)}, \tag{71}$$

where $\#\text{ass. frames}_{\mathrm{AR,GT}}$ is the number of frames containing at least one correspondence between a *GT* and an *AR* object. Using the frame count of the sequence according to the definition in [33] would give empty scenes an occluding influence on the value of this measure. $\#\mathrm{FIT}(j)$ and $\#\mathrm{FIO}(j)$ are the number of FIT and FIO, respectively, in frame $j$ according to the definitions of (60) and (61).

## 4.7. Event detection measures

The most important step for event detection measures is the matching of *GT* data and *AR* data, which can be

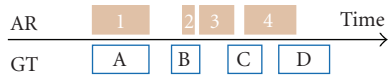


Figure 14: Time-line of events. What is the best matching between events?

solved by simple thresholding. Most of the proposals in the literature match events by using the shortest time delay between the events in *GT* and *AR*. In the event that the time delay exceeds a certain threshold, matching fails. This is a reliable approach for simple scenarios with few events. However, considering real world scenarios, this approach does not return the correct match. A simple example is depicted in Figure 14, where one match might be A-1, B-2, and C-4 and a second one might be A-1, B-2, C-3, D-4, among other possible matches. Desurmont et al. [39] propose a dynamic realignment algorithm using dynamic programming to compute the best match between *GT* and *AR* events. The algorithm incorporates a maximum allowed delay between events.

The CREDS project [40] classifies correct detection into three categories: *perfect*, *anticipated,* and *delayed*. Each event in the *GT* data may be associated to a single correct detection. Multiple overlaps in time are not covered in detail, the first occurrence is matched and the remaining events are treated as *FP*. The authors define a score function of delay/anticipation and a ratio between *GT* event duration ($\mathrm{GT_{ed}}$) and *AR* event duration ($\mathrm{AR_{ed}}$):

$$S_{\mathrm{CD}}(t,\mathrm{AR_{ed}},\mathrm{GT_{ed}}) = \begin{cases} 0, & (t < B) \vee (t > D), \\ \dfrac{S}{A-B}(t-B), & B \le t \le A, \\ S, & A \le t \le 0, \\ \dfrac{S}{D}(D-t), & 0 \le t \le D. \end{cases} \tag{72}$$

$S$ represents the maximum score associated with a correct detection. The authors compute it as follow:

$$S = \begin{cases} 50 * \left[2 - \left(1 - \dfrac{\mathrm{AR_{ed}}}{\mathrm{GT_{ed}}}\right)^2\right], & 0 \le \dfrac{\mathrm{AR_{ed}}}{\mathrm{GT_{ed}}} \le 2, \\ 50, & \dfrac{\mathrm{AR_{ed}}}{\mathrm{GT_{ed}}} > 2. \end{cases} \tag{73}$$

The maximum tolerated delay is expressed by $D$ in milliseconds, whereas $A$ represents the accepted anticipation in milliseconds. $B$ stands for the maximum tolerated anticipation in milliseconds. The values $D$, $A$, and $B$ are dependent on the event type (warning event, alarm event, or critical event).

The ETISEO [15] project defined a set of metrics for events to. Measures for correctly detected events over the whole sequence are defined. In the first set of event detection measures M5.1.1, only whether events occurred is compared and not their time of occurrence nor object association. Time constraints are added to M5.1.1 in the second measure set M5.1.2. A last set of measures M5.3.1 is defined which facilitates correct detection in time and parameters. Parameters are object classes, so called contextual zones (areas such as a street, a bus stop) and involved physical objects. For instance, an event "car parked in forbidden zone" has to be raised once a physical object, which has been classified as car, is idle for longer than a defined time interval in a contextual zone which is marked as "no parking area." The formulas for measures M5.1.1, M5.1.2, and M5.3.1 are defined identically, only the matching criteria are different. $\mathrm{Prec_{event}}$, $\mathrm{Sens_{event}}$, and $\mathrm{F\text{-}Score_{event}}$ are used by ETISEO [15]:

$$\begin{aligned} \mathrm{Prec_{event}} &= \frac{\#\mathrm{TP}_e}{\#\mathrm{TP}_e + \#\mathrm{FP}_e}, \\ \mathrm{Sens_{event}} &= \frac{\#\mathrm{TP}_e}{\#\mathrm{TP}_e + \#\mathrm{FN}_e}, \\ \mathrm{F\text{-}Score_{event}} &= \frac{2 \cdot \mathrm{Prec_{event}} \cdot \mathrm{Sens_{event}}}{\mathrm{Prec_{event}} + \mathrm{Sens_{event}}}. \end{aligned} \tag{74}$$

*TP* relates to a match between *GT* and *AR*.

#### 4.7.1. Chosen event detection measure subset

We choose M5.1.2 defined in [15] with the dice coefficient (21) for the matching of the time intervals as event detection metric:

(i) $\mathrm{Prec_{event\,TI}}$,

(ii) $\mathrm{Sens_{event\,TI}}$,

(iii) $\mathrm{F\text{-}Score_{event\,TI}}$.

### 4.8. Object classification measures

Senior et al. [10] propose the measure *Object type error* which simply counts the number of tracks with incorrect classification. The definition is somewhat vague as it is unknown if a track has to be classified more than fifty percent of the time correctly to be treated as correctly classified. ETISEO [15] uses different measures classes. A simple class (M4.1.1) uses the number of correctly classified physical objects of interest in each frame. The second measure class (M4.1.2) matches, in addition to M4.1.1, the bounding boxes of the objects. ETISEO distinguishes between misclassifications caused by classification shortcomings and misclassifications caused either in the object detection or the classification step:

$$\mathrm{Prec_{class}} = \frac{\#\mathrm{TP}_c}{\#\mathrm{TP}_c + \#\mathrm{FP}_c}, \tag{75}$$

$$\mathrm{Sens_{class}} = \frac{\#\mathrm{TP}_c}{\#\mathrm{TP}_c + \#\mathrm{FN}_c}, \tag{76}$$

$$\mathrm{Sens_{class,det}} = \frac{\#\mathrm{TP}_c}{\#\mathrm{TP}_c + \#\mathrm{FN}_{c,\mathrm{det}}}, \tag{77}$$

$$\mathrm{F\text{-}Score_{class}} = \frac{2 \cdot \mathrm{Prec_{class}} \cdot \mathrm{Sens_{class}}}{\mathrm{Prec_{class}} + \mathrm{Sens_{class}}}, \tag{78}$$

$$\mathrm{F\text{-}Score_{class,det}} = \frac{2 \cdot \mathrm{Prec_{class}} \cdot \mathrm{Sens_{class,det}}}{\mathrm{Prec_{class}} + \mathrm{Sens_{class,det}}}. \tag{79}$$

$\#TP_c$ refers to the number of objects types classified correctly. $\#FN_c$ is the number of false negatives caused by classification shortcomings, for example, unknown class, $\#FN_{c,\text{det}}$ refers to the number of false negatives, caused by object detection errors or by classification shortcomings.

In M4.1.3, the measures in M4.1.2 are enhanced by the ID persistence criteria. $\text{Prec}_{\text{class}}$, $\text{Sens}_{\text{class}}$, and $\text{F-Score}_{\text{class}}$ are computed and used as measure. Due to the separation between misclassifications, two $\text{Sens}_{\text{class}}$ and $\text{F-Score}_{\text{class}}$ measures are defined in each measure class. The measures in M4.1.1 through M4.1.3 are computed at frame level. Percentages for a complete sequence are computed as follows. The sum of percentages per image divided by the number of images containing at least one *GT* object.

$\text{Prec}_{\text{class}}$, $\text{Sens}_{\text{class}}$, and $\text{F-Score}_{\text{class}}$ are computed per object type in M4.2.1. Therefore, the number of measures equals the number of existing object types. The time percentage of good classification is computed in M4.3.1:

$$\frac{\left|\text{GT}_d \cap \text{AR}_d, \text{Type}(\text{AR}_d) = \text{Type}(\text{GT}_d)\right|}{\left|\text{GT}_d \cap \text{AR}_d\right|}. \tag{80}$$

$\text{GT}_d$ relates to the time interval in *GT* data, whereas $\text{AR}_d$ relates to the time interval in *AR* data. Nghiem et al. [34] suggest to use M4.1.2.

#### 4.8.1. Chosen classification measure subset

*Class correctness rate (CCR)*

Assesses the percentage of correctly classified objects. Therefore, the types of the objects, which are assigned to each other by the assignment step described in context of the detection measures, are compared and the correct and false classifications are counted:

$$\text{CCR} = \frac{1}{\#\text{ass. frames}_{\text{AR,GT}}} \sum_j \frac{\#\text{CC}(j)}{\#\text{CC}(j) + \#\text{FC}(j)}, \tag{81}$$

where $\#\text{CC}(j)$ and $\#\text{FC}(j)$ are the number of correctly, respectively, falsely classified objects in frame $j$, and $\#\text{ass. frames}_{\text{AR,GT}}$ is the number of frames containing at least one correspondence between *GT* and *AR* objects.

We also use a metric according to ETISEO's M4.2.1, which consists of two different specifications. The first considers only the classification shortcomings and the other includes the shortcomings of the detection to. With the first specification, we agree, leading to the definition in (75), (76), and (78).

*Object classification performance by type*

(i) $\text{Prec}_{\text{class}}$ (75),

(ii) $\text{Sens}_{\text{class}}$ (76),

(iii) $\text{F-Score}_{\text{class}}$ (78).

In the second specification, we differ from ETISEO because we also take *FP* objects into account.

*Object detection and classification performance by type*

$$\begin{aligned}
\text{Prec}_{\text{class,det}} &= \frac{\#\text{TP}_c}{\#\text{TP}_c + \#\text{FP}_{c,\text{det}}}, \\
\text{Sens}_{\text{class,det}} &= \frac{\#\text{TP}_c}{\#\text{TP}_c + \#\text{FN}_{c,\text{det}}}, \\
\text{F-Score}_{\text{class,det}} &= \frac{2 \cdot \text{Prec}_{\text{class}} \cdot \text{Sens}_{\text{class,det}}}{\text{Prec}_{\text{class}} + \text{Sens}_{\text{class,det}}},
\end{aligned} \tag{82}$$

where, in contrast to (75), $\text{FP}_{c,\text{det}}$ is used as the number of false positives caused by shortcomings in the detection or classification steps.

### 4.9. 3D object localization measures

3D object localization measures are defined in [15]. The average, variance, minimum, and maximum of distances between objects in *AR* as well as the trajectories of the objects in *GT* are computed. Object gravity centers are used to calculate the distances.

*Average of object gravity center distance (AGCD) [15]*

Measures the average of the distance between gravity centers in *AR* and *GT*:

$$d_i = \left|\left|\text{TOC}_{\text{GT}}(i) - \text{TOC}_{\text{AR}}(i)\right|\right|_2, \qquad \text{AGCD} = \frac{1}{N}\sum_i^N d_i, \tag{83}$$

where $\text{TOC}(i)$ is the trajectory of the object's center of gravity at time $i$ and $N$ is the amount of elements.

*Variance of object gravity center distance (VGCD) [15]*

Computes the variance of the distance between gravity centers in *AR* and *GT*:

$$\text{VGCD} = \frac{1}{N}\sum_i^N (d_i - \text{AGCD})^2. \tag{84}$$

*Minimum and maximum distance of object gravity centers (MIND, MAXD) [15]*

Considers the minimum distance between centers of gravity in *AR* and *GT*:

$$\text{MIND} = \inf\{d \in D\}, \qquad \text{MAXD} = \sup\{d \in D\}, \tag{85}$$

where $D$ is the set of all $d_i$. Nghiem et al. [34] state that detection errors on the outline are not taken into account in [15]. Moreover there is no consensus on how to compute the 3D gravity center of certain objects, like cars.

Note that when evaluating 3D information inferred from 2D data, the effects of calibration have to be taken into account. If both *AR* and *GT* are generated from 2D data and projected into 3D, the calibration error will be systematic.

If the *GT* is obtained in 3D, for example, using a differential global positioning system (DGPS), and the *AR* still generated from 2D images, then the effects of calibration errors have to be taken into account.

### 4.10. Multicamera measures

Tracking across different cameras includes identifying an object correctly in all views from different cameras. This task, and possibly a subsequent 3D object localization (Section 4.9), are the only differences to tracking within one camera view only. Note that an object can be in several views from different cameras at once, or it can disappear from one view to appear in the view of another camera some time later. The most important measure to quantify the object identification is the ID persistence (64), which can be evaluated for each view separately once the *GT* is labeled accordingly and averaged afterwards. Again, the averaging has to be chosen carefully, just as in the computation of measures within one camera view (Section 4.11). Multicamera measures applying tracking measures (Section 4.6) using 3D instead of 2D coordinates have been proposed for specific applications such as tracking football players [41] or objects in traffic scenes [42].

### 4.11. The problem of averaging

At different stages during the computation of the measures, single results of the measures are combined by averaging. Within one frame, for example, the values for different objects may be merged into one value for the whole frame. The single frame-based values of the measures are then aggregated to gain a value for the whole sequence. These sequence-based values are again combined for a subset of examined sequences to one value for each metric.

Regarding the performance profile for a set of different sequences, it has to be known which averaging strategy was used for the aggregation of the measures. The chosen averaging strategy may tip the scales of the resulting measure value. In the following sections, several issues concerning the different averaging steps are highlighted.

#### 4.11.1. Averaging within a frame

The metrics concerning object localization (Section 4.5) are an example for the combination of measure values of several objects to an aggregated value for one frame. The unique assignment as used for the strict detection measures (Section 4.4.2) provides a basis for the computation here. For each *GT* object to which an *AR* object was assigned, a value exists for the corresponding metric. Concerning the averaging, two different possibilities exist. Either the unassigned *GT* objects get the worst value of zero for not being localized and the averaging is done via the number of *GT* objects, or only the existing assignments are considered and the averaging and normalization is done via their number.

The first approach has the disadvantage of placing too much emphasis on the detection performance and thus masking the localization effects. A bad detection rate would thus decrease the values of the localization significantly. The second approach favors algorithms which detect only a few objects but do so precisely. Algorithms, which find objects which are hard to detect and localize precisely, are at a disadvantage here. This disadvantage could be avoided by using only these *GT* objects which were detected by both algorithms in the averaging for the algorithm comparison.

#### 4.11.2. Averaging within a sequence

Basically, there are two ways to combine object-based measures for a sequence. One is to calculate a total value for each *GT* track and then to average over all *GT* tracks. The other way is to average the frame-wise results into one total value for the whole sequence.

##### Averaging by track values

On the one hand, localization metrics for example do not have to be combined frame-wise only, as described above. They can be combined track-wise as well. In this case, each measure is averaged over the lifetime of the track. Similar to averaging frame-wise, time instants, when the corresponding track cannot be assigned, have different effects on the averaging. On the other hand, there are pure track-based measures such as track coverage rate (68) or track fragmentation resistance (69). On averaging track values, the way in which *FN* tracks, which are *GT* tracks that are never assigned to an *AR* track, are handled has to be considered in both cases. Identical conclusions have to be drawn as for frame-wise averaging regarding *FN* objects mentioned above.

##### Averaging by frame values

Calculating an average value of a metric for the whole sequence can be done in various ways. An important factor in this is mainly the number of frames to average over. Which way is more meaningful depends on the corresponding metric. The problem is that for certain measures there is not necessarily a defined value in all frames. For a frame, which has no *GT* object, there is no value for example for detection sensitivity. In parallel, there is no value for detection precision for a frame lacking an *AR* object. As a result of this, there is no value for the F-Score for frames not featuring values for sensitivity nor precision. One way to handle this is to define missing values, that is, assuming an optimal value of 1 and dividing the sum of all frame values by the number of frames in the sequence. As consequence, these values would prefer sequences with only objects appearing for a short duration. Another method is to sum up values and divide by the number of frames, showing at least on *GT* object [15]. This is an appropriate approach for those metrics that can only be calculated when a *GT* object exists, as for the detection sensitivity. There are drawbacks in this approach for other metrics. The value for detection precision is also defined in frames, not showing a *GT* object. It is defined as 0. This results in *FP* objects being excluded from the

averaging of the detection precision in frames not showing a *GT* object. Such a method would result in strict detection precision (38) and lenient detection precision (Section 4.4.2) being incapable of representing an increase or decrease of *FP* objects in empty scenes when comparing two algorithms. This is not an issue when dividing by the number of frames with *AR* objects in these situations, instead of using the number of frames with *GT* objects. A deterioration of values for detection precision as predicted can be ensured, when *AR* objects are falsely detected in frames not showing *GT* objects. Accordingly, the sum of all F-Score values has to be divided by the number of frames showing at least one *GT* object or at least one *AR* object.

#### 4.11.3. Averaging over a collection of sequences

The single performance profiles for different sequences have to be combined in the last step to an overall profile for a sequence subset. The obvious approach is to sum the sequence values for each measure and divide by the number of sequences. The disadvantage is that the value of each sequence is weighted the same for the overall value. As the sequences differ greatly in length, number of *GT* objects, and level of difficulty, this distorts the overall result. An extreme example is a sequence with 200 000 frames and numerous challenges for the algorithm being weighted the same as a sequence with 200 frames showing only some disturbers, but no objects of interest. For the latter, even one *FP* object leads to a detection precision of zero. Combining these two sequences equally weighted leads to a performance profile which does not represent the performance of the algorithm appropriately.

To avoid these effects, weights could be assigned to the sequences and included in the computation of the averaging. However, a sensible choice of the weighting factors is neither easy nor obvious. A second possibility is the purposeful selection of sequence subsets for which the averaging of the measure values results in an adequately representative result.

## 5. EVALUATION

The above-mentioned metrics provide information about various aspects of the system's performance. As indicated already, it is usually not possible to draw conclusions concerning the differences in performance of two algorithms by means of a single measure without considering the interplay of interdependent measures. This section also shows how to recognize strengths and weaknesses of an algorithm by means of the metrics chosen in Section 4. Therefore, considering various performance aspects, relevant combinations of different metrics are listed and their evaluation is explained starting with general remarks about measure selection (Section 5.1) and sequence subsets (Section 5.2).

The ATE (Section 3) is generally used to compare performances of different versions of the video surveillance systems in the development stage. Usually, two different versions are chosen and their results compared. On the one hand, this happens graphically by means of bar charts featuring predefined subsets of calculated measures. Evaluating these so-called performance profiles is described by means of two examples in Section 5.3. One the other hand, a statistical evaluation is done as will be described in Section 5.4. The metrics used in the ATE (Section 3) are all normalized, so at evaluation time they can all be treated alike. This simplifies the statistical evaluation of results as well as their visualization.

### 5.1. Selecting and prioritizing measures

After having presented measures for each stage of a surveillance system such as segmentation (Section 4.3), object detection (Section 4.4), object localization (Section 4.5), tracking (Section 4.6), event detection (Section 4.7), object classification (Section 4.8), 3D object localization (Section 4.9), and multicamera tracking (Section 4.10), is there any importance ranking between the different families of measures? What are the most reliable measures for an end-user? Is there a range or threshold for some or all measures which qualifies a surveillance system to be "good enough" for a user? The only general answer to these questions is that it usually depends on the chosen task.

#### 5.1.1. Balancing of false and miss detections

In assessing detection rates by means of precision and sensitivity, for example, it was assumed that false and miss detections are equally spurious. Based on this assumption, the F-Score was used as a balancing measure. In fact, depending on the application either *FP*s or *FN*s can represent a greater problem.

Concerning live alarming systems, *FP*s are at least distracting, since too many false alarms distract security personnel. Consequently, parameterization makes the system less sensitive to keep the false alarm rate low, thus accepting missed events. For retrieval applications, *FP*s are less problematic, because they can be identified and discarded quickly. *FN*s, on the other hand, would diminish the benefit of the retrieval system and are therefore especially spurious.

In these cases, the F-Score is less useful, because nonequal weighting of precision and sensitivity is necessary. The F-Measure provides a solution for the discussed drawback by adjusting the weighting.

#### 5.1.2. Priority selection of measures

Depending on the performance aspect to be assessed, the measures are also examined with different priorities. The end-user may be interested in a specific event in a well-defined scene, for example, "intrusion: detect an object going through a fence from a public into a secure area" or "check if there are more than 15 objects in the specified area at the same time." In scenarios like these, the end-user is most interested in best performance regarding event detection measures (detect all events without any false positives). In comparison of different surveillance systems, the one with the best event detection results is preferred. This is how i-LIDS [7] benchmarks their participants.

For a developer of an existing system, the event measures may be too abstract to get an insight if a small algorithm change; a new feature or a different parameter set has improved the system. Depending on the modification, the most significant measure may be that for detection, localization or tracking, or a combination of all of them.

In the case of evaluating, for example, the performance of an algorithm for perimeter protection, it is first and foremost important how many of the intruders are detected in relation to the amount of false alarms. The values of the event detection measures $\text{Prec}_{\text{event}}$, $\text{Sens}_{\text{event}}$, and $\text{F-Score}_{\text{event}}$ with respect to the event "Intrusion" are of most significance here.

In a next step, false positive and false negative track resistance (FPTR and FNTR), as well as the frame-based alarm correctness rate (ACR), can be regarded. All other measures, like the different detection or segmentation measures, are only of interest if more precise information is asked for. As a rule, this is the case if the coarse-granular results are scrutinized. A meaningful evaluation for this task would thus cover the above-mentioned measures as well as some fine-granular like detection measures to support the results further.

In the case of a less specific evaluation task, the usual procedure is to start with coarse-granular measures and to proceed to the more fine-granular measures. That means that, similar to the example of perimeter protection above, first of all the event detection measures are regarded, continuing with tracking measures, which express whether complete tracks were missed or falsely detected. The next level is object based and includes the detection measures, which express how well the detection of objects over time is done. The finest level corresponds to pixel-based analysis of the algorithm behavior and includes the segmentation and object localization measures. Here, it is not analyzed whether the objects are detected, but how well the detection is done in terms of localization and precise segmentation.

The measures within the above-mentioned granularity levels can be again prioritized from elemental measures to others describing more detailed information. The tracking measures, for example, can be structured by the following aspects.

(i) A track was found (FNTR).

(ii) Duration of the detected track (TCR).

(iii) Continuity of the tracking (TFR, OP, FITR, ...).

This is also motivated by the observation of dependencies between different measures. An example is track fragmentation resistance (TFR) and track coverage rate (TCR). A value indicating a good track fragmentation resistance becomes less significant if the track coverage rate is bad because the TFR is based on only a few matches. If the TFR changes for the better, but the TCR for the worse, then it can be assumed that the tracking performance deteriorates.

A complete prioritization of the presented measures is still an open issue. It is a big challenge as the definition of good performance depends often on the chosen task. The amount of measures and their interdependencies further complicate the prioritization.

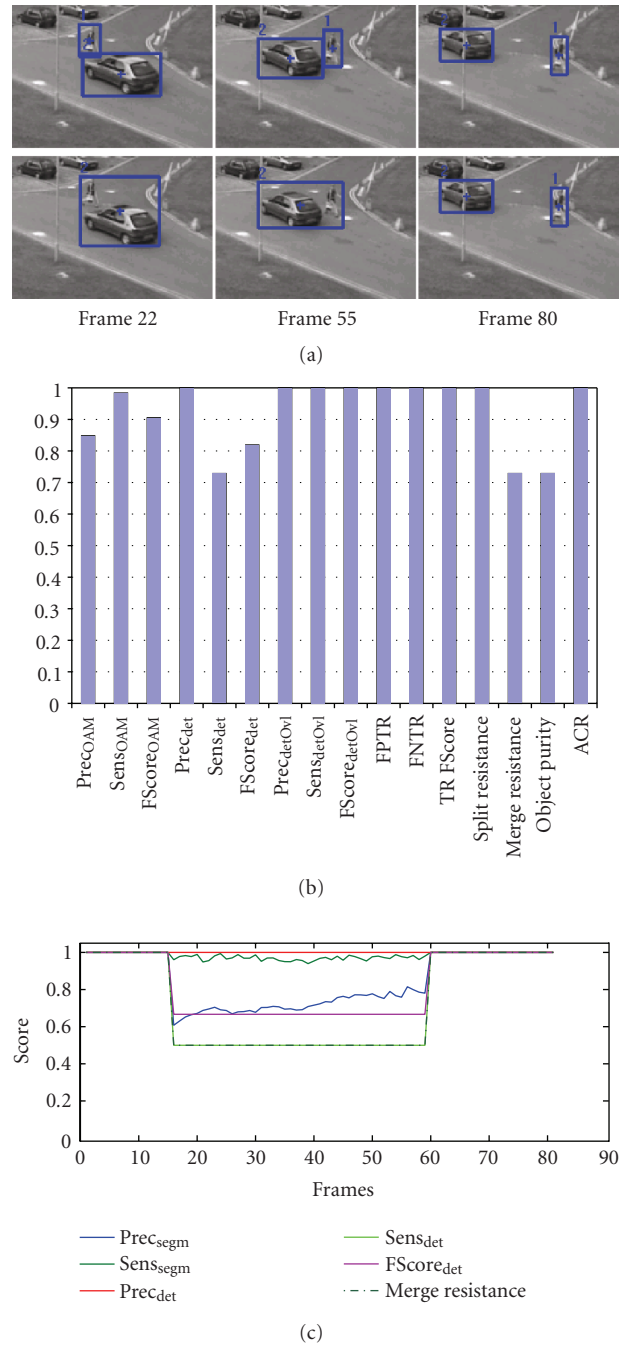


Figure 15: Example 1: crossing of a person and a car, an extract from the PETS 2001 training dataset 1. Simulation of algorithm deficit by merging the two objects. (a) Three screen shots from the sequence with bounding boxes of *GT* (top) and results of simulated detection algorithm (bottom) added. (b) The performance profile of the simulated algorithm result. (c) The temporal development of selected measures displays selected measure values for each frame.

Table 2: Observations (F1–F6) of the behavior of the measures in the performance profile shown in Figure 15(b). Out of these observations, the above listed assumptions (A1–A3) of the algorithm performance can be made.

| | |
|---|---|
| F1 | $\text{Sens}_{\text{OAM}}$ is nearly maximal, but $\text{Prec}_{\text{OAM}}$ is only around 0.85 |
| F2 | The strict detection measures behave the other way round: $\text{Prec}_{\text{det}}$ is maximal, but $\text{Sens}_{\text{det}}$ is approximately 0.7 |
| F3 | The lenient detection measures are maximal |
| F4 | *FP* track resistance (FPTR) and *FN* track resistance (FPTR) are maximal |
| F5 | Merge resistance is about 0.7 |
| F6 | Object purity is about 0.7 |
| A1 | F1, F3, F4<br>no regions with activity were overlooked |
| A2 | F2, F3, F5<br>some objects were not separated but merged. This can be derived directly from the nonoptimal values of the merge resistance. The observation is confirmed by the strict $\text{Sens}_{\text{det}}$ being nonoptimal in contrast to the lenient $\text{Sens}_{\text{detOvl}}$ |
| A3 | F6<br>at least one *GT* object is not being tracked correctly for a significant amount of time |

### 5.2. Sequence subsets for scenario evaluation

As described in Section 2.3, it is important to establish the results using an appropriate sequence subset. In the case of perimeter protection, for example, it is of no use to evaluate the algorithms using sequences containing scenarios from a departure platform. Then, the performance of the algorithm will depend on acquisition conditions as well as sequence content, both containing more or less challenging situations. For a better evaluation of the algorithms, dividing the sequences into subsets and analyzing each condition separately are often necessary.

Furthermore, different parameter settings might be used in the system for day and night scenarios, or other acquisition conditions. Then, the algorithm should be evaluated for each of these scenarios separately on representative sequence sets. However, in practice, the surveillance system will either run on one parameter set the whole time, or it will need to determine the different conditions itself and switch the parameters automatically. Therefore, a wide variety of acquisition conditions need to be evaluated for an overall behavior of the system.

In the ATE, the algorithms are evaluated on all available sequences. For the evaluation task, individual subsets of these sequences can then be chosen for deeper investigations of algorithm performance.

### 5.3. Performance profiles

Parallel visualization of multiple measure values represents the performance profile for one or several aspects for the different algorithm versions simultaneously. The bars of the resulting measures of the two versions to be compared are always arranged next to each other. This method immediately highlights to improvements or deterioration. Evaluating the performance profile requires experience, since the metrics are subject to certain dependencies. Isolated observation of some measures, for example, regarding precision without sensitivity, is thus not very reasonable either.

Due to the amount of different measures, displaying them all together in a performance profile is not feasible. For a specific evaluation task, typically only a certain subset is of interest. For example, a developer who is interested in evaluating changes to a tracking algorithm does not want to regard classification measures. Therefore, a preselection of measures to be displayed is usually done.

To demonstrate how metrics reflect the weaknesses of algorithms, two short sections of the well-known PETS 2001 dataset [8] were chosen and typical errors like merging and disturbance regions were simulated by labeling them. From the manually generated *AR* data and the corresponding *GT*, selected measures were computed and will be analyzed in the following.

#### 5.3.1. Example 1: reading performance profiles

Figure 15(a) shows the first simple example from the PETS 2001 training dataset 1, where the passing of a car and a person can be seen. Here, it is simulated that the video analysis system is not capable of tracking both objects separately but rather merging them into a single object.

Usually, the measures are regarded without knowing which errors the algorithm has made. With the help of a performance profile (see Figure 15(b)), the performance and shortcomings of the algorithm can be analyzed. Thus, the task is to draw conclusions concerning the algorithm behavior out of the observed measures. For our example, the observations and subsequent assumptions can be found in Table 2.

The temporal development of the measures (Figure 15(c)) displays effectively the frames in which measures are affected. The upward trend of the curve representing $\text{Prec}_{\text{OAM}}$ is mostly due to the effects of the approximation using the bounding box. At the beginning of the merge, a large bounding box is spanned over both

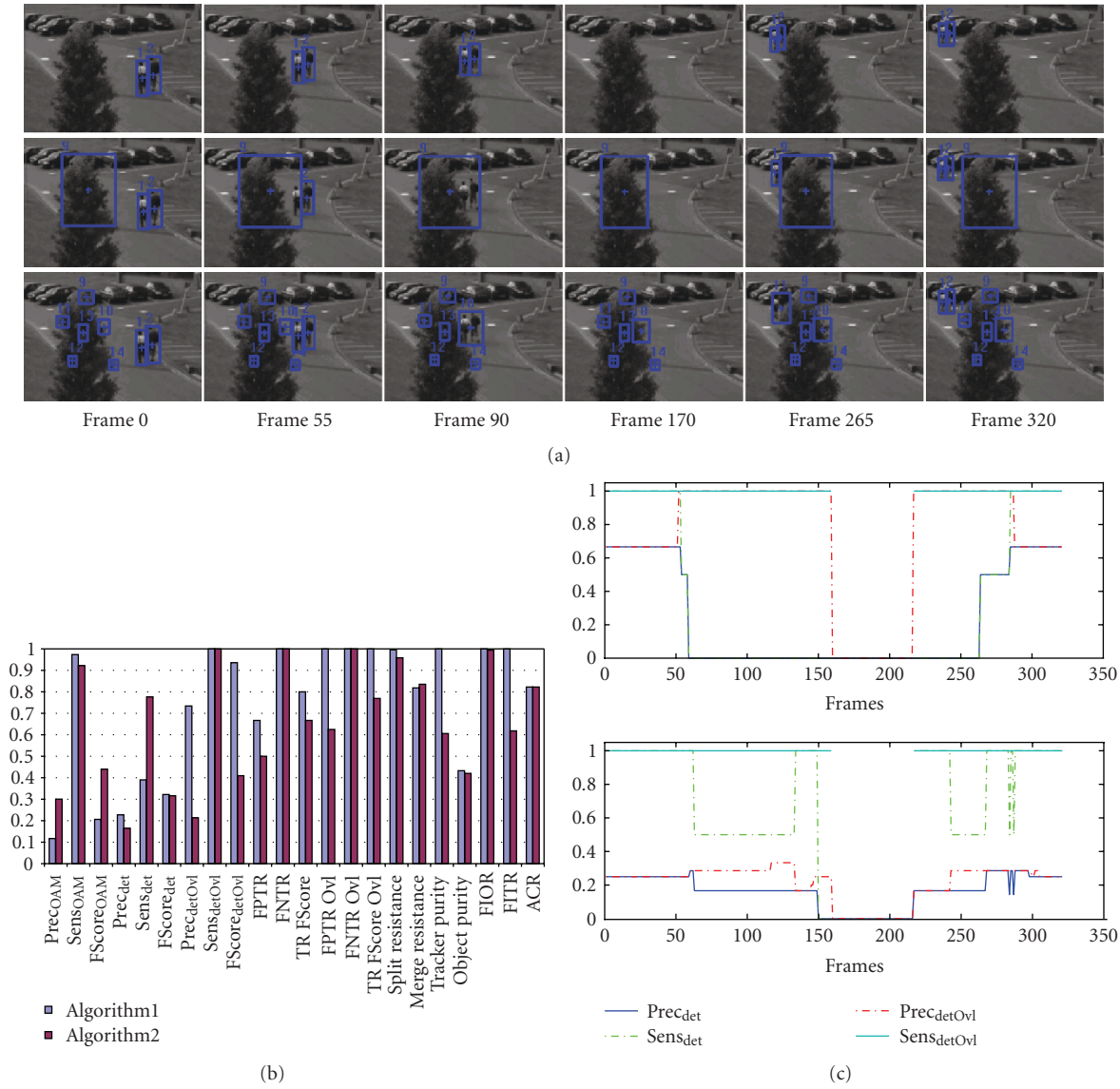


FIGURE 16: Example 2: two people crossing a waving tree, extract from the PETS 2001 testing dataset 3. Simulation of two algorithms coping differently with the movement of the tree and generating false detections there. (a) Screen shots from the sequence with bounding boxes of *GT* (top) and the results of Algorithm 1 (middle) and Algorithm 2 (bottom) added. (b) Performance profile of the two simulated algorithms visualized in parallel to compare the overall measures for them. (c) The temporal development of selected measures for Algorithm 1 (top) and Algorithm 2 (bottom) displays selected measure values for each frame.

car and person. This bounding box shrinks successively, and thus also the segmented space between the two *GT* objects which caused the bad values of $\text{Prec}_{\text{OAM}}$.

### 5.3.2. *Example 2: comparing performance profiles*

Example 1 (Section 5.3.1) shows a case in which algorithm errors are successfully identified via their effects on the chosen measures. In practice, it is usually not so simple. When several objects occur simultaneously in a sequence, the complexity grows rapidly. Example 2 (see Figure 16(a)) shows an extract from the PETS 2001 testing dataset 3, in which two people walk past a moving tree. In contrast to the last example, two different, fictive algorithm versions are compared here. The algorithms differ in their reaction to the moving tree. The first algorithm detects the moving tree continuously as one single large object, and the second algorithm finds six small objects in the region of the tree. Note that the tree should not be detected at all.

Examining the corresponding performance profile (see Figure 16(b)), several facts can be observed and lead to the hypotheses in Table 3. Based on these statements, assumptions of the changes between the two algorithm versions can be made. First of all, the presence of permanent disturbances can be assumed (A1 and A2) for both algorithms. For Algorithm 2, more *AR* objects result from the disturbance

Table 3: Observations (F1–F10) on the behavior of the measures in the performance profiles shown in Figure 16(b). Algorithm 1 is used as reference version, and the changes to Algorithm 2 are described. Out of the observations, the above listed assumptions (A1–A7) of the algorithm performances can be made.

| | |
|---|---|
| F1 | $\text{Prec}_{\text{OAM}}$ is on a low level, but significant improvements can be seen, whereas $\text{Sens}_{\text{OAM}}$ is near maximum but decreases slightly |
| F2 | $\text{Prec}_{\text{det}}$ is on a low level and deteriorates further, whereas $\text{Sens}_{\text{det}}$ nearly doubles to 0.8 |
| F3 | $\text{Prec}_{\text{detOvl}}$ drops from a high level to low values, and $\text{Sens}_{\text{detOvl}}$ is maximal in both cases |
| F4 | Strict *FP* track resistance (FPTR) starts from a middle level and degrades significantly, while the strict *FN* track resistance (FNTR) is maximal in both cases |
| F5 | The lenient *FP* track resistance (FPTR Ovl) drops from maximum to mid-level |
| F6 | Merge resistance, which is considerably lower than maximum, improves slightly |
| F7 | Tracker purity drops from maximum to mid-level |
| F8 | Object purity is on a middle level and changes only marginal |
| F9 | FIT resistance (FITR) drops from maximum to mid-level |
| F10 | The alarm correctness rate (ACR) stays unchanged at around 0.8 |
| A1 | F3, F10<br>in about 20 percent of the frames, objects are detected though none are contained in the *GT*. No alarm case has been overlooked as $\text{Sens}_{\text{detOvl}}$ is maximal |
| A2 | F4<br>no *GT* track has been overlooked |
| A3 | F1, F4, F5<br>the amount of *FP* tracks is increased. Instead of some large objects, there are now more smaller objects, as $\text{Prec}_{\text{OAM}}$ has grown |
| A4 | F3, F4, F5<br>all *FP* objects of Algorithm 1 touch for at least one frame a *GT* Objekt, whereas this is not the case for Algorithm 2 as the lenient *FP* track resistance is not maximal there |
| A5 | F2, F3, F4, F10<br>for a large amount of the sequence there exist *FP* objects as the detection rate is on a low level and the strict *FP* track resistance at middle values |
| A6 | F2, F8, F9<br>the detection rate is enhanced because of additional *AR* objects which correspond to *GT* objects |
| A7 | F7<br>the additional *AR* objects (A5) of Algorithm 2 only have short correspondences to *GT* objects in comparison to their lifetime |

region but collectively, they are smaller in comparison to Algorithm 1 (A3). The fundamental problem of Algorithm 1, the alarm status being wrong for 20 percent of the frames (A5), is still in existence for Algorithm 2. The seemingly significant improvement of $\text{Sens}_{\text{det}}$ is due to coincidental correspondences to the disturbance objects (A6, A7) and no real performance enhancement of the algorithm. This conclusion is confirmed by the fact that $\text{F-Score}_{\text{det}}$ is equal for both algorithms.

The performance profile used for this example with a short sequence, and only one challenge is already quite complex and not easy to evaluate. Considering the case of an evaluation over a large number of sequences at once, it becomes obvious that, due to blending and compensation effects of algorithm peculiarities, it is even more difficult to draw conclusions about the change between two versions of an algorithm. Here, statistical analysis as provided by the ATE, for example, information about which sequences have the largest changes for distinct measures, can help. Would a change like the one of $\text{Sens}_{\text{det}}$ in Example 2 occur in the statistics, a next step would be to take a specific look at the performance profile of this sequence and at the temporal progress of $\text{Sens}_{\text{det}}$ and other relevant measures for further analysis.

Regarding the temporal progress curves in Figure 16(c), it can be seen that $\text{Prec}_{\text{det}}$ is never maximal for the whole sequence for both algorithms. This indicates the presence of *FP* objects for the duration of the whole sequence. Furthermore, the temporal range in the middle of the sequence, where both algorithms have problems, attracts attention immediately as well as the time slots where Algorithm 2 performed better than Algorithm 1 for $\text{Sens}_{\text{det}}$. This explains the strong improvement of the average value of this measure for Algorithm 2.

A next step could be to look at the frames in which errors were identified, with *GT* and *AR* bounding boxes overlaid, to find the real cause of the problem. This approach is especially helpful if the sequence is too long to view it completely at a reasonable expenditure of time.

### 5.4. Automatic evaluation

The procedure described in Section 5.3.2 for comparing two ATE passes by manually comparing their performance

profiles is applicable as long as the focus is on only a few different sequences or all sequences are similar and not all measures are included into the evaluation process. If the evaluation commences on a rather large set of different sequences and the amount of relevant measures cannot be limited preliminarily, this evaluation method will be very laborious. This is where automatic statistical arrangements support in pointing out significant differences and in visualizing them. ATE output answering for example the following questions can be considered.

(i) Which measure changed most significantly on average?

(ii) Which sequences show most changes?

(iii) Which sequences feature the best or worst results for a certain measure?

(iv) How many sequences show improvements, how many show deterioration?

Automatic profile evaluation can also support qualitative statements such as the following.

(i) "The current version is more sensitive than the reference version."

(ii) "The current version is more capable of detecting objects separately than the reference version."

(iii) "The current version is less sensitive to disturbances."

Very often it can be observed that optimization of the algorithm resulting in improvements for certain sequences has a negative impact on other sequences. Averaging the measure values over all kinds of sequences may lead to compensational effects which distort the impression of the changes. Therefore, it is better to categorize sequences into subsets which are then evaluated separately. Another way is to have the ATE cluster single sequences by certain features and providing statements such as: "64 percent of the sequences featuring illumination changes have fewer false alarms." Meaningfully sorted arrangements give a quick overview on which performance differences two compared versions of the algorithm have. Furthermore, they provide starting points for thoroughly inspecting the results. For frame-based measures, for example, the temporal progress of the measures for single sequences can be examined next, including looking at interesting parts of the video by means of *GT* and *AR* bounding boxes drawn into the frame.

## 6. SUMMARY AND CONCLUSION

This paper presents an overview of surveillance video algorithm performance evaluation. Starting with environmental issues like ground truth generation (Section 2.2) and the choice of a representative benchmark data set to test the algorithms (Section 2.3), a complete evaluation framework has been presented (Section 3). The choice of the benchmark data set is of great importance as the explanatory power of the measures is not retained for a badly arranged compilation of the sequences.

The automated test environment (ATE, Section 3) aids developers in getting a general idea of the performance of an algorithm via an overview of the measures for a group of sequences. Furthermore, it aids in systematically finding critical regions within a single sequence to examine specific behavioral details of algorithms. However, the test environment can only be used sensibly if the user has an accurate knowledge of the employed measures as well as their interactions. Important questions are, for example, what does a specific measure actually measure, and how are the measure values combined. Computational details have to be considered for these questions as well. It is not possible to appropriately describe the performance of an algorithm with only one measured value though, for specific algorithms, emphasis can be laid on single measures by assigning them larger weights in their aggregation.

For a better understanding of surveillance video algorithm performance metrics published in the literature, an exhaustive overview together with an discussion of their usefulness has been given (Section 4). The definitions of these measures often differ only marginally or even not at all. The differences can usually be found in the implementation details like using different averaging strategies. These computational details are of crucial importance for the resulting measure values. However, they are often documented insufficiently. An example is the assignment of *AR* and *GT* objects (Section 4.2), which is an important step in the computation of many measures and should be implemented with particular care. Here, uniqueness and comprehensibility are of significance. Special attention has also been given to the problem of averaging measures within the frames as well as over one or several sequences (Section 4.11) as this has a large impact on the expressiveness of the computed measures.

Out of the results of the analysis of the measures and the presentation of desirable modifications, a subset of expedient measures is proposed for the thorough analysis of video algorithm performances. Evaluation of measures has been done exemplarily for two simple scenarios, the first analyzing a performance profile of a merge of a car and a person (Section 5.3.1), and the second analyzing the differences in the performance of two different fictional algorithms coping with two people walking past a moving tree (Section 5.3.2). Even for these simple examples, the derivation of the algorithm peculiarities out of the regarded measures is a challenging task. When the sequences are longer, or a large set of sequences is regarded, the interactions of the different phenomena and effects on the measures become quite complex. Therefore, statistical analysis for systematic detection and evaluation of regions of interesting algorithm behavior in complex scenarios has been introduced (Section 5.4).

With this paper, a better understanding of evaluating video surveillance system performance is propagated by increasing the comprehension of the properties and peculiarities of hitherto published measures and the computational and environmental details which have a large impact on the evaluation results. Attention is brought to these details to encourage researchers to document them properly when describing the performance of their algorithms. Thus, the

comparability of published algorithms is also augmented as the understanding of the different measures used for their evaluations allows a better judgement of their performance.

## REFERENCES


[1] H. Dee and S. Velastin, "How close are we to solving the problem of automated visual surveillance? A review of real-world surveillance, scientific progress and evaluative mechanisms," *Machine Vision and Applications*. In press.

[2] F. Porikli, "Achieving real-time object detection and tracking under extreme conditions," *Journal of Real-Time Image Processing*, vol. 1, no. 1, pp. 33–40, 2006.

[3] CAVIAR, "Context aware vision using image-based active recognition," http://homepages.inf.ed.ac.uk/rbf/CAVIAR/.

[4] CLEAR, "Classification of events, activities and relationships—evaluation campaign and workshop," http://www.clear-evaluation.org/.

[5] CREDS, "Call for real-time event detection solutions (creds) for enhanced security and safety in public transportation," http://www.visiowave.com/pdf/ISAProgram/CREDS.pdf.

[6] ETISEO, "Video understanding evaluation," http://www-sop.inria.fr/orion/ETISEO/.

[7] i-LIDS, "Image library for intelligent detection systems," http://scienceandresearch.homeoffice.gov.uk/hosdb2/physical-security/detection-systems/i-lids/.

[8] IEEE International Workshop on Performance Evaluation of Tracking and Surveillance (PETS), http://pets2007.net/.

[9] VACE, "Video analysis and content extraction," http://www.perceptual-vision.com/vt4ns/vace_brochure.pdf.

[10] A. Senior, A. Hampapur, Y. Tian, L. Brown, S. Pankanti, and R. Bolle, "Appearance models for occlusion handling," in *Proceedings of the IEEE International Workshop on Visual Surveillance and Performance Evaluation of Tracking and Surveillance (VS-PETS 01)*, Kauai, Hawaii, USA, December 2001.

[11] J. Black, T. Ellis, and P. Rosin, "A novel method for video tracking performance evaluation," in *Proceedings of the IEEE International Workshop on Visual Surveillance and Performance Evaluation of Tracking and Surveillance (VS-PETS 03)*, pp. 125–132, Nice, France, October 2003.

[12] L. M. Brown, A. W. Senior, Y. Tian, J. Connell, and A. Hampapur, "Performance evaluation of surveillance systems under varying conditions," in *Proceedings of the 2nd Joint IEEE International Workshop on Visual Surveillance and Performance Evaluation of Tracking and Surveillance (VS-PETS 05)*, Beijing, China, October 2005.

[13] D. P. Young and J. M. Ferryman, "PETS metrics: on-line performance evaluation service," in *Proceedings of the 2nd Joint IEEE International Workshop on Visual Surveillance and Performance Evaluation of Tracking and Surveillance (VS-PETS 05)*, pp. 317–324, Beijing, China, October 2005.

[14] S. Muller-Schneiders, T. Jager, H. S. Loos, and W. Niem, "Performance evaluation of a real time video surveillance system," in *Proceedings of the 2nd Joint IEEE International Workshop on Visual Surveillance and Performance Evaluation of Tracking and Surveillance (VS-PETS 05)*, vol. 2005, pp. 137–143, Beijing, China, October 2005.

[15] ETISEO, "Internal technical note metrics definition—version 2.0," 2006, http://www.silogic.fr/etiseo/iso_album/eti-metrics_definition-v2.pdf.

[16] A. T. Nghiem, F. Bremond, M. Thonnat, and R. Ma, "A new evaluation approach for video processing algorithms," in *Proceedings of the IEEE Workshop on Motion and Video Computing (WMVC 07)*, p. 15, Austin, Tex, USA, February 2007.

[17] C. E. Erdem, B. Sankur, and A. M. Tekalp, "Performance measures for video object segmentation and tracking," *IEEE Transactions on Image Processing*, vol. 13, no. 7, pp. 937–951, 2004.

[18] T. List and R. B. Fisher, "CVML—an XML-based computer vision markup language," in *Proceedings of the 17th International Conference on Pattern Recognition (ICPR 04)*, vol. 1, pp. 789–792, Cambridge, UK, August 2004.

[19] PETS metrics on-line evaluation service, http://www.petsmetrics.net/.

[20] ViPER, "The video performance evaluation resource," http://viper-toolkit.sourceforge.net/.

[21] T. Ellis, "Performance metrics and methods for tracking in surveillance," in *Proceedings of the 3rd IEEE International Workshop on Visual Surveillance and Performance Evaluation of Tracking and Surveillance (VS-PETS 02)*, pp. 26–31, Copenhagen, Denmark, June 2002.

[22] G. R. Taylor, A. J. Chosak, and P. C. Brewer, "OVVV: using virtual worlds to design and evaluate surveillance systems," in *Proceedings of the IEEE Computer Society Conference on Computer Vision and Pattern Recognition (CVPR 07)*, pp. 1–8, Minneapolis, Minn, USA, June 2007.

[23] M Nilsback and A. Zimmerman, "Delving into the whorl of flower segmentation," in *Proceedings of the British Machine Vision Conference*, Warwick, UK, September 2007.

[24] T. List, J. Bins, J. Vazquez, and R. Fisher, "Performance evaluating the evaluator," in *Proceedings of the 2nd Joint IEEE International Workshop on Visual Surveillance and Performance Evaluation of Tracking and Surveillance (VS-PETS 05)*, pp. 129–136, Beijing, China, October 2005.

[25] AVITrack, "Aircraft surroundings, categorised vehicles & individuals tracking for apron's activity model interpretation & check," http://www.avitrack.net/.

[26] C. Jaynes, S. Webb, R. Steele, and W. Xiong, "An open development environment for evaluation of video surveillance systems," in *Proceedings of the 3rd IEEE International Workshop on Visual Surveillance and Performance Evaluation of Tracking and Surveillance (VS-PETS 02)*, pp. 32–39, Copenhagen, Denmark, June 2002.

[27] CANDELA, "Content analysis and network delivery architectures," http://www.hitech-projects.com/euprojects/candela/.

[28] T. Fawcett, "An introduction to ROC analysis," *Pattern Recognition Letters*, vol. 27, no. 8, pp. 861–874, 2006.

[29] N. Lazarevic-McManus, J. Renno, G. A. Jones, et al., "Performance evaluation in visual surveillance using the F-measure," in *Proceedings of the 4th ACM International Workshop on Video Surveillance and Sensor Networks*, pp. 45–52, Santa Barbara, Calif, USA, October 2006.

[30] F. Bashir and F. Porikli, "Performance evaluation of object detection and tracking systems," in *Proceedings of the 9th IEEE International Workshop on Visual Surveillance and Performance Evaluation of Tracking and Surveillance (VS-PETS 06)*, New York, NY, USA, June 2006.

[31] N. Lazarevic-McManus, J. Renno, D. Makris, and G. Jones, "Designing evaluation methodologies: the case of motion detection," in *Proceedings of the 9th IEEE International Workshop on Visual Surveillance and Performance Evaluation of Tracking and Surveillance (VS-PETS 06)*, pp. 23–30, New York, NY, USA, June 2006.

[32] V. Manohar, P. Soundararajan, H. Raju, D. Goldgof, R. Kasturi, and J. Garofolo, "Performance evaluation of object

detection and tracking in video," in *Proceedings of the 7th Asian Conference on Computer Vision (ACCV 06)*, vol. 3852 of *Lecture Notes in Computer Science*, pp. 151–161, Hyderabad, India, January 2006.

[33] K. Smith, D. Gatica-Perez, J. Odobez, and S. Ba, "Evaluating multi-object tracking," in *Proceedings of the IEEE Computer Society Conference on Computer Vision and Pattern Recognition (CVPR 05)*, vol. 3, p. 36, San Diego, Calif, USA, June 2005.

[34] A. T. Nghiem, F. Bremond, M. Thonnat, and V. Valentin, "ETISEO, performance evaluation for video surveillance systems," in *Proceedings of the IEEE Conference on Advanced Video and Signal Based Surveillance (AVSS 07)*, pp. 476–481, London, UK, September 2007.

[35] P. Correia and F. Pereira, "Objective evaluation of relative segmentation quality," in *Proceedings of the IEEE International Conference on Image Processing (ICIP 00)*, vol. 1, pp. 308–311, Vancouver, Canada, September 2000.

[36] Y. Zhang, "A review of recent evaluation methods for image segmentation," in *Proceedings of the 6th International Symposium on Signal Processing and Its Applications (ISSPA 01)*, vol. 1, pp. 148–151, Kuala Lumpur, Malaysia, August 2001.

[37] J. C. Nascimento and J. S. Marques, "Performance evaluation of object detection algorithms for video surveillance," *IEEE Transactions on Multimedia*, vol. 8, no. 4, pp. 761–774, 2006.

[38] C. Needham and R. Boyle, "Performance evaluation metrics and statistics for positional tracker evaluation," in *Proceedings of the 3rd International Conference on Computer Vision Systems (ICVS 03)*, pp. 278–289, Graz, Austria, April 2003.

[39] X. Desurmont, R. Sebbe, F. Martin, C. Machy, and J.-F. Delaigle, "Performance evaluation of frequent events detection systems," in *Proceedings of the 9th IEEE International Workshop on Visual Surveillance and Performance Evaluation of Tracking and Surveillance (VS-PETS 06)*, New York, NY, USA, June 2006.

[40] F. Ziliani, S. Velastin, F. Porikli, et al., "Performance evaluation of event detection solutions: the CREDS experience," in *Proceedings of the IEEE International Conference on Advanced Video and Signal Based Surveillance (AVSS 05)*, pp. 201–206, Como, Italy, September 2005.

[41] Y. Li, A. Dore, and J. Orwell, "Evaluating the performance of systems for tracking football players and ball," in *Proceedings of the IEEE International Conference on Advanced Video and Signal Based Surveillance (AVSS 05)*, pp. 632–637, Como, Italy, September 2005.

[42] R. Spangenberg and T. Döring, "Evaluation of object tracking in traffic scenes," in *Proceedings of the ISPRS Commission V Symposium on Image Engineering and Vision Metrology (IEVM 06)*, Dresden, Germany, September 2006.